

# 1 Annual time-series 1-km maps of crop area and types in the 2 conterminous US (CropAT-US): ~~cropping~~Cropping diversity 3 changes during 1850-2021

4 Shuchao Ye, Peiyu Cao, Chaoqun Lu

5 Department of Ecology, Evolution, and Organismal Biology, Iowa State University, Ames, Iowa 5011, USA

6 Correspondence: Chaoqun Lu (clu@iastate.edu)

7 **Abstract.** Agricultural activities have been recognized as an important driver of land ~~use and cover changes~~  
8 (~~LUC~~/land use change (LCLUC) and have significantly impacted ~~the~~ ecosystem feedback to climate, ~~air, and water~~  
9 ~~quality~~ by altering land surface properties. A reliable historical cropland distribution dataset is crucial for  
10 understanding and quantifying the legacy effects of agriculture-related ~~LUC~~LCLUC. While several ~~LUC~~LCLUC  
11 datasets have the potential to depict cropland patterns in the conterminous US, there remains a dearth of a ~~relatively~~  
12 high-resolution dataset with crop type details over a long period. To address this gap, we reconstructed historical  
13 cropland density and crop type maps from 1850 to 2021 at a resolution of 1 km×1 km by integrating ~~county-level~~  
14 ~~crop-specific~~ inventory datasets, ~~census data~~, and gridded ~~LUC~~LCLUC products. ~~Different from other databases,~~  
15 ~~we tracked the planting area dynamics of all the crops in the US, excluding idle/fallow farm land, and cropland pasture.~~  
16 The results showed that the ~~developed dataset is~~crop acreages for nine major crops derived from our map products are  
17 highly consistent with the county-level inventory data, with ~~an  $R^2$  approaching one and RMSE~~the residual less than ~~3~~  
18 ~~Mha (million 0.2 thousand hectares) at (Kha) in most counties (>75%) during the national-level entire study period.~~  
19 Temporally, the US total crop acreage has increased by 118 million hectares (Mha) from 1850 to 2021, primarily  
20 driven by corn (30 Mha) and soybean (35 Mha). Spatially, the hotspots of cropland ~~distribution~~ shifted from Eastern  
21 US to the Midwest and the Great Plains, and the dominant crop types (corn and soybean) ~~moved toward the Northwest~~  
22 ~~of the US, expanded northwestward.~~ Moreover, we found the US cropping ~~system~~ diversity experienced a significant  
23 increase from 1850s to 1960s, followed by a dramatic ~~decrease~~decline in the recent six decades under the intensified  
24 agriculture. Generally, ~~the~~this newly developed dataset could facilitate the spatial data development in delineating  
25 crop-specific management practices and enable the quantification of cropland change impacts.

Formatted: Font: Not Italic

## 26 1 Introduction

27 Anthropogenic land ~~use and cover~~/land use change (~~LUCC~~LULUC) has altered nearly 70% of global ice-free  
28 land (Arnell et al., 2019), exerting significant effects on ecosystem services by changing biogeochemical and  
29 biophysical processes (Foley et al., 2005; Goldewijk et al., 2017; Johnson, 2013; Betts et al., 2007; Lark, 2023). In  
30 particular, agricultural activities have been identified as the dominant driver of ~~LUCC~~LULUC (Cao et al., 2021), with  
31 approximately one-third of the land surface altered for agricultural use to meet human demands of food, feed, fiber,  
32 and fuel (Zhang et al., 2007). These changes have led to a range of environmental issues, including greenhouse gas  
33 emissions (De Noblet-Ducoudré et al., 2012; Yu et al., 2018), agricultural water pollution (Ouyang et al., 2014), and  
34 soil degradation (Vanwallegem et al., 2017). In addition, the intensification of agriculture causes the decline of crop  
35 diversity, which can reduce the resilience of crops to various environmental stresses and threaten the crop yield  
36 (Burchfield et al., 2019; Gaudin et al., 2015; Renard and Tilman, 2019; Aizen et al., 2019). Therefore, gaining a better  
37 understanding of spatiotemporal cropland extent and type changes is critical to quantify the environmental effects of  
38 cropland change and promote sustainable agricultural practices (Tilman et al., 2011; Lambin and Meyfroidt, 2011).

39 As a leading agricultural producer, the conterminous US has experienced a substantial transformation in crop area,  
40 distribution, and type over the last two centuries. From 1850s to 1980s, the crop area increased about eightfold from  
41 around 20 million hectares to about 160 million hectares, primarily through the conversion of forest, grassland, and  
42 other land types (Li et al., 2023; Turner, 1988). Spatially, the development of canals, waterways, and railroads  
43 contributed to the cropland expansion to the west (Meinig, 1993). Especially, the Homestead Acts in 1862 played a  
44 significant role in stimulating agricultural reclamation. Moreover, in crop commodities, the dominant crop types have  
45 shifted. Before the mid-twentieth century, corn and wheat were the dominant crops. However, the cultivated area of  
46 soybean has gradually surpassed wheat and became the second widely produced crop type across the US in recent  
47 decades (Lubowski et al., 2006). Although these changes have been reported by the government and social scientists  
48 (Waisanen and Bliss, 2002), there is still a lack of a long-term cropland dataset to depict the ~~historical crop-specific~~  
49 spatial patterns ~~of crop type choice and distribution~~ in the US ~~over a long time period~~. Despite that long-term crop-  
50 specific management information has been available in the US for quite a long period, large uncertainties remain in  
51 developing historical management maps and assessing their environmental and economic consequences spatially,  
52 because not knowing “what is planted where” is a big hurdle before the remote sensing data is available.

53 A wide variety of land use datasets have been used to explore the spatiotemporal patterns of agricultural land in  
54 the contiguous US. For instance, History database of global environment (HYDE) (Goldewijk et al., 2017) ~~dataset~~  
55 ~~provides the cropland area in each grid cell from 1000 BC to 2017 AD at a resolution of 5 arc-min. constructed a~~  
56 ~~weighting algorithm involving dynamical social (historical population density and national/sub-national crop statistics,~~  
57 ~~state level crop inventory in US) and stable environmental (soil suitability, temperature, and topography) factors to~~  
58 ~~reconstruct the historical crop distribution at the resolution of 5 arc-minute~~. Similarly, Zumkehr and Cambell (2013)  
59 ~~developed a cropland distribution dataset at a 5 arc-min resolution from 1850 to 2000. adopted a land-use model of~~  
60 ~~Romankutty and Foley (Ramankutty and Foley, 1999) and a satellite-derived cropland distribution map to calculate~~  
61 ~~the historical crop area grid by grid under the control of crop inventory records~~. Although these datasets present the  
62 long-term land use change history, their coarse resolutions offer limited spatial details. ~~In contrast, the resolution~~

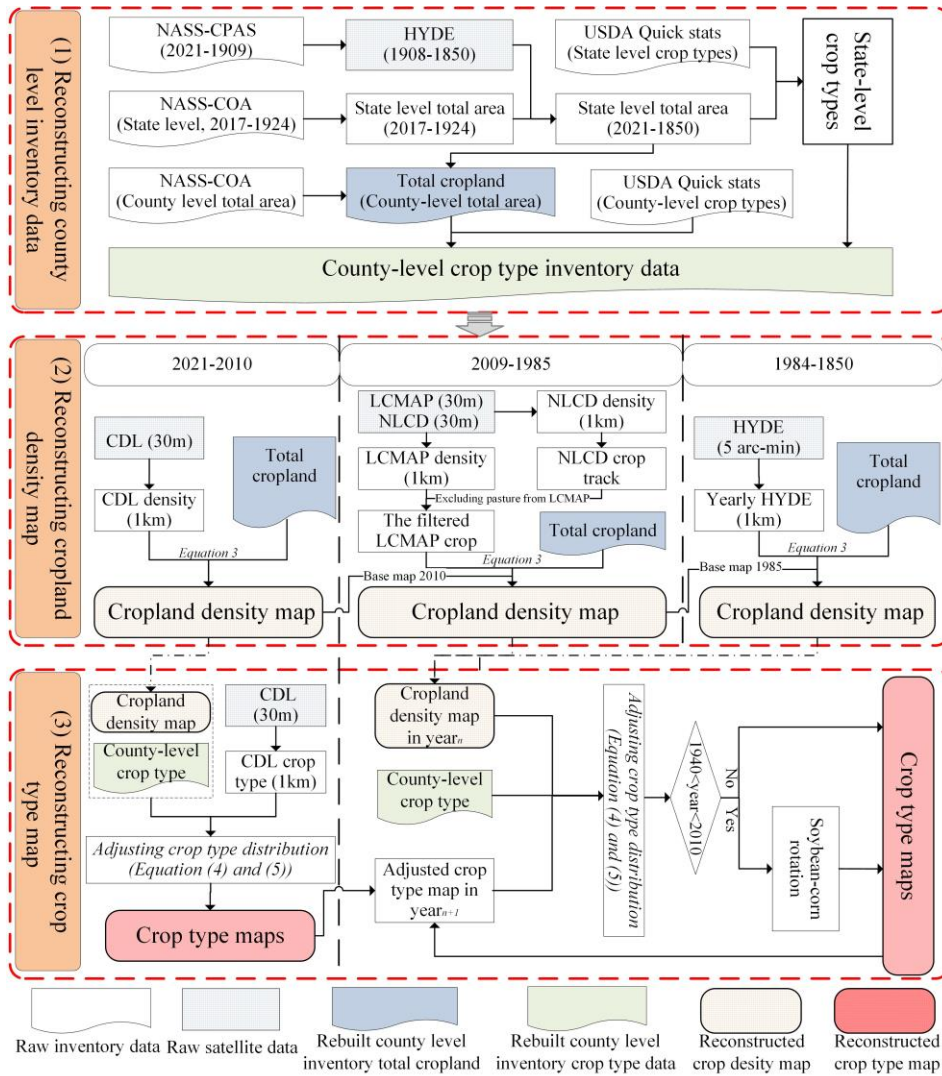
63 ~~of~~Growing remote sensing technology and machine learning methods enhance the capability to monitor land surface  
64 ~~change with the high resolution LCLUC products (Tian et al., 2014; Shi et al., 2020). For instance,~~ Cropland Data  
65 Layer (CDL), National Land Cover Database (NLCD), and Land Change Monitoring, Assessment, and Projection  
66 (LCMAP) ~~is down to 30m. However, their availability and continuity (available in the recent 40 years) are unable to~~  
67 ~~provide historical cropland change patterns. The more recent studies, such as Cao et al. provide the gridded cropland~~  
68 ~~distribution maps at the resolution of 30m by 30m (Homer et al., 2020; Xian et al., 2022; Lark et al., 2017). However,~~  
69 ~~these high-resolution datasets lack the capability to depict historical cropland change patterns before the emergence~~  
70 ~~of satellite images. Recently, Cao et al. (2021) and Li et al. harmonized cropland demands from HYDE and Land-Use~~  
71 ~~Harmonization 2 datasets with the combination of cropland suitability, kernel density, and other constraints to generate~~  
72 ~~a cropland dataset from 10000 BCE to 2100 CE. Li et al. (2023), developed long-term LUCC datasets integrated an~~  
73 ~~artificial neural network-based probability of occurrence estimation tool and multiple inventories to generate the~~  
74 ~~historical cropland maps at 1-km-by-1-kmthe resolution, but of 1km by 1km. However, the crop type details are still~~  
75 ~~missing in these datasets, making it challenging to recognizeidentify the specific crop type change over space and~~  
76 ~~time. On the other hand, Monfreda et al. (2008) and Tang et al. combined a global cropland dataset and multi-level~~  
77 ~~census statistics (national, state, and county) to generate a map depicting the area and yield of 175 crops circa the year~~  
78 ~~2000 around the world, and Tang et al. (2023) generated a global crop type map with more than 170 crop types~~  
79 ~~in further updated it to depict 173 crops circa the year of 2000 and 2020, and CDL provides the annual crop type~~  
80 ~~distribution in the conterminous US with more than 50 crop types from 2008 to now. Their products also provide~~  
81 ~~information that is only available in the recent two decades, hindering the limiting our understanding forof historical~~  
82 ~~US crop type development. Overall, the currently available datasets either have short periods, low spatial resolution,~~  
83 ~~or lack specific crop type information, which makes it impossible to assess. This limits our capability in assessing~~  
84 ~~how crop type changes and crop-specific management before 2000 have affected the climate system and~~  
85 ~~environmental quality at a finer scale. Thus, it is urgent to develop a long-term spatially explicit cropland dataset with~~  
86 ~~crop type details to comprehend the historical US cropland changesUS agricultural land use history.~~

87 In this study, we aim to reconstruct the cropland density and crop type maps in the conterminous US from 1850  
88 to 2021 at 1 km by 1 km resolution. The cropland density ~~map presents~~maps present the distribution and percentage  
89 of ~~planted~~crop planting area in each 1 km by 1 km pixel. The crop type ~~map displays~~maps display the distribution of  
90 nine major crop types (corn, soybean, winter wheat, spring wheat, durum wheat, cotton, sorghum, barley, and rice)  
91 and one ~~type of~~category labeled as “others” (including all remaining crop types but excluding idle/fallow farm land,  
92 and cropland pasture). This study consists of three sections: Section 2 describes the materials and methods used to  
93 reconstruct the dataset, Section 3 analyzes the spatiotemporal changes in dominant crop types and ~~erof~~cropping  
94 diversity based on the reconstructed dataset, and Section 4 discusses the differences between our dataset and other  
95 datasets, the drivers of cropland change, the implications of US crop diversity change, and the data uncertainty.

## 96 2 Materials and method

97 In this study, we combined three inventory datasets and four gridded datasets to reconstruct the historical cropland  
98 density and crop type maps. As illustrated in Figure 1, the entire process involves three stages: reconstructing annual

99 inventory data for each crop type at the county level (Section 2.2), rebuilding cropland density maps (Section 2.3),  
100 and generating crop type maps (Section 2.4). In particular, we adopted the following assumptions for reconstructing  
101 the cropland maps: (1) the USDA inventory datasets provide the most reliable acreage information for determining  
102 cropland area in each county; (2) Cropland data layer (CDL), History database of the global environment 3.2 (HYDE)  
103 (Goldewijk et al. 2017), and Land change monitoring, assessment, and projection (LCMAP) provide the potential  
104 distribution of cropland, which ~~are~~were used to allocate cropland grids under the control of the rebuilt inventory data  
105 (Yu and Lu, 2018); (3) The rotation percentage between corn and soybean ~~linearly-increased~~remained constant when  
106 the rotation information was unavailable from 1940 to 2009. ~~The method for acquiring the rotation ratio is introduced~~  
107 ~~in Section 2.4.~~ Furthermore, based on the generated crop type maps, we explored the historical US crop diversity  
108 pattern through the ~~diversity index~~.true diversity index (Jost, 2006).



109  
 110 Figure 1. The methodology flow chart. Three boxes with red dashed lines correspond to Section 2.2, 2.3, and 2.4,  
 111 respectively. The county-level total and crop-specific cropland area generated in the box (1) are fed into box (2) and  
 112 box (3) to reconstruct cropland density and crop type maps, respectively. (NASS-CPAS: Crop Production Annual  
 113 Summary data from Nation agricultural statistical service of USDA; NASS-COA: Census of Agriculture from Nation  
 114 agricultural statistical service of USDA; CDL: Cropland data layer; NLCD: National land cover database; LCMAP:  
 115 Land change monitoring, assessment, and projection; HYDE: History database of the global environment 3.2  
 116 (Goldewijk et al. 2017).

## 117 2.1 Datasets

118 ~~Three inventory datasets and four gridded LUCC datasets are used in this study (Table 1). Specifically, NASS-~~  
119 ~~CPAS (Crop Production Annual Summary data from the Nation agricultural statistical service of USDA) and NASS-~~  
120 ~~COA (Census of Agriculture from Nation agricultural statistical service of USDA) provide the total cropland area in~~  
121 ~~each state and each county. USDA NASS Quickstat is used to track the acreage of specific crop types. These inventory~~  
122 ~~datasets are adopted to reconstruct the historical cropland area. CDL is the most detailed satellite-based cropland~~  
123 ~~dataset, which has been intensively validated by ground truths and other ancillary data with crop classification~~  
124 ~~accuracies up to 90% for major crop commodities (Boryan et al., 2011). Here, we extracted the above mentioned ten~~  
125 ~~crop types from CDL (Table S1). CDL 2008 and 2009 were excluded due to their low resolution and accuracy~~  
126 ~~compared to other years (Johnson, 2013). NLCD and LCMAP, all derived from Landsat images with a resolution of~~  
127 ~~30m×30m, were used to provide the cropland spatial information from 1985 to 2009. More specifically, NLCD~~  
128 ~~provides around 5-year cyclical land cover maps from 2001 to 2019, and LCMAP offers annual land use data from~~  
129 ~~1985 to 2021 (Homer et al., 2020; Xian et al., 2022). Since the cropland in LCMAP includes cropland and pasture,~~  
130 ~~we applied the NLCD-based cropland trajectory to exclude pasture grids in LCMAP (more details presented in~~  
131 ~~Supplementary Methods). HYDE was adopted to offer the potential cropland distribution during 1850–1984. All~~  
132 ~~gridded datasets were resampled to 1km.~~

133 Three inventory datasets and four gridded LCLUC datasets were used in this study (Table 1). Specifically, NASS-  
134 CPAS (Crop Production Annual Summary data from the Nation agricultural statistical service of USDA) and NASS-  
135 COA (Census of Agriculture from Nation agricultural statistical service of USDA) provide the total cropland area in  
136 each state and each county. USDA-NASS Quickstat was used to track the acreage of specific crop types. These  
137 inventory datasets were adopted to reconstruct the historical crop-specific planting area for each county from 1850 to  
138 2021, which served as a benchmark for adjusting the spatial maps in terms of planting acreage. CDL is the most  
139 detailed satellite-based cropland dataset for the period of 2010–2021, which has been intensively validated by ground  
140 truths and other ancillary data with crop classification accuracies up to 90% for major crop commodities (Boryan et  
141 al., 2011; Yu and Lu, 2018). Here, we extracted ten crop types (Table S1) from CDL. We compared the planting area  
142 between inventory data and CDL for nine crop types across counties from 2010 to 2021 (Figure S1). For most counties  
143 (>75%), the residuals (the inventory-based crop area minus CDL-based crop area) are less than 10 Kha for durum  
144 wheat while they are less than 5 Kha for other crops. NLCD and LCMAP, both derived from Landsat images with a  
145 resolution of 30m×30m, were integrated to provide the spatial information of cropland distribution from 1985 to 2009.  
146 NLCD crop area is highly consistent with CPAS and COA, except that the crop area was significantly underestimated  
147 in NLCD 1992 (Figure 4 in Yu and Lu, 2018), so it was excluded for reconstructing historical crop maps (Johnson,  
148 2013). Due to its consistency in cropland area, we utilized NLCD for identifying the spatial distribution of cropland  
149 (Homer et al., 2020). However, NLCD provides around 5-year cyclical land cover maps from 2001 to 2019 (Homer  
150 et al., 2020). LCMAP offers annual land use data from 1985 to 2021. LCMAP adopts Anderson Level I-based legend,  
151 grouping cropland and pasture into one category (Xian et al., 2022). In contrast, NLCD uses a Level II-based legend  
152 where cropland and pasture are separately tracked (Xian et al., 2022) (Table S4). To generate a reliable cropland  
153 distribution, the long-term non-crop trajectory derived from NLCD was used to exclude all grids identified as cropland

154 the LCMAP map (more details are presented in Supplementary Methods: (1) Preprocesses for LCMAP). For the period  
 155 of 1850-1984, although both ZCMAP and HYDE provide the cropland distribution, HYDE considers the impacts of  
 156 various environmental factors (soil suitability, temperature, and topography) on crop distribution compared with  
 157 ZCMAP (Goldewijk, 2001; Goldewijk et al., 2011; Goldewijk et al., 2017; Zumkehr and Campbell, 2013).  
 158 Consequently, HYDE (available every 10 years) was initially used to identify the cropland distribution by calculating  
 159 the fraction of cropland to the physical area for each grid. We further linearly interpolated the fraction for the missing  
 160 years between two available years to provide a potentially continuous cropland distribution (more details are presented  
 161 in (2) Linear interpolation in HYDE of Supplementary Methods). All gridded datasets were resampled to 1km. We  
 162 employed a 1km\*1km window to aggregate the total cropland area from the 30m\*30m map and assigned the area to  
 163 the corresponding 1km\*1km grid. To resample the CDL crop type map from 30m to 1km, the crop type in each 1km  
 164 by 1km pixel was assigned to the dominant crop type with the largest fraction of land area within the 1km\*1km  
 165 window. Conversely, the cropland percentage in each 5 arc-min grid is interpolated to 1km\*1km grid cells with an  
 166 assumption that cropland percentage is evenly distributed within the 5 arc-min by 5 arc-min window.

167 Table 1. The gridded and inventory dataset sources.

Data variables (period, resolution)	Properties	Adjustment
CDL (2010-2021, 30m)	The most detailed crop type <del>map</del> maps. Providing info of crop type and distribution.	Resampled to 1km and reclassified into ten crop types (nine major crop types and one type of “others”).
LCMAP (1985-2021, 30m)	Anderson Level I-based legend classification including eight primary land types (Xian et al., 2022). The cropland includes cropland and pasture.	Filtering pasture from cropland based on NLCD crop trajectory.
NLCD (2001-2019, 3-5 years intervals, 30m)	Anderson Level II-based legend including 20 land cover classes (Xian et al., 2022).	Providing cropland distribution.
HYDE 3.2 (1600-2017, 5arc-min)	Including cropland, grazing land, pasture, irrigated rice, etc. Providing cropland distribution.	<del>Linearly</del> Linear interpolation in missing years (1850-1985) (Equation S2).
NASS-CPAS (1909-2021)	State-level total <del>planted</del> planting area-of major principal crops*.	Gap-filling in missing years (Section 2.2).
NASS-COA (1924-2017, 4-5 years intervals)	State and county-level total cropland area of harvest, failure, and fallow crops.	Gap-filling in missing years (Section 2.2).
USDA-NASS Quickstat (1866-2021)	State and county level <del>planted</del> crop-specific planting and <del>harvest</del> harvesting area. Including corn, soybean, winter	Gap-filling in missing years (Section 2.2).

Formatted Table

wheat, spring wheat, durum wheat,  
cotton, sorghum, barley, rice, and all  
other crop types.

\* Principal crops refer to grains, hay, oilseeds, cotton, tobacco, sugar crops, dry beans, peas, lentils, potatoes, and miscellaneous crops.

## 2.2 Reconstructing historical crop acreage history at the county level

By integrating and gap-filling multiple inventory and gridded datasets, we reconstructed the total cropland county-  
level time series of planting area and the planting area of 9 for nine major crop types in each state and other crops from  
1850 to 2021. We obtained Our reconstruction process was initiated with the area of “others” by calculating the  
development of crop-  
specific planting areas at the state level. NASS-CPAS reports the annual plant total planting area of all principal major  
crops for each state from 1909 to 2021, which excludes. However, some minor crop types (, such as vegetables and  
fruits), are excluded. USDA-COA provides the total area areas of crop harvest, failure, and fallow for each state from  
1925 to 2017 with 4~5-year intervals. We computed the difference between these two datasets for available years and  
linearly interpolated unavailable years during 1909-2021. The difference was assumed to be the planting area of those  
minor crops. The interpolated difference was then added back to NASS-CPAS to generate the annual state-level total  
crop plant planting area of all crops from 1909 to 2021. We used the interannual variations of arable land of each state  
extracted from HYDE to interpolate extrapolate the total planting area during 1850 from 1908 to 1850 (Equation 1).

To identify the planting acreage change for nine major crop types, we obtained the state-level harvest crop-  
specific harvesting and plant planting area from USDA-NASS Quickstat. The available harvest harvesting and  
plant planting areas vary among crop types and states, for which the harvest harvesting areas usually have earlier-year  
reports than those of planting areas (Table S2). The harvest harvesting area is highly correlated to plant planting area  
in terms of interannual variation. We calculated the ratio of plant planting area to harvest harvesting area for the earliest  
available year of plant planting area. We then converted the harvest harvesting areas to plant planting areas by timing  
the ratio with the harvest harvesting areas to extend the plant planting areas to an earlier period. For the period that the  
harvest harvesting areas are unavailable, we interpolated the plant planting area from 1850 to 2021 based on the total  
cropland planting area generated above (as a referenced trend. Equation 1 and was used when only the beginning or  
the ending year of the period is available, while Equation 2)- was used when both beginning and ending years are  
available. The planting area of “others” was obtained by calculating the difference between the total planting area and  
the summation of planting area of 9 major crops.

We adopted the same approach as for the state-level plant planting area generated above to obtain the county-level  
total cropland planting area and the planting area of 9 major crop types and “others”. USDA-COA reports the total  
county cropland area from 1925 to 2017 with 4~5-year intervals. We gap-filled the total county cropland planting  
area from 1850 to 2021 by using state total cropland planting area (as a referenced trend (using Equation 1 for gap-  
filling in cases where only beginning or ending year is available and Equation 2); in cases where both beginning and  
ending years are known). Similar to the state-level crop-specific planting area, we converted the harvest harvesting

Formatted: Comment Reference

Formatted: Comment Reference



201 areas to ~~plant~~planting areas of ~~9~~nine major crops in each county from USDA-NASS Quickstat, with varied availability  
 202 (Table S1). For the period when ~~harvest~~harvesting areas are unavailable, we gap-filled the ~~plant~~planting areas of each  
 203 ~~crop~~ during 1850-2021 based on the state-level crop-specific ~~plant~~planting area generated above as a ~~referenced trend~~  
 204 (Equation 1 and 2). The ~~plant~~planting area of all other crops (“others”) in each county was estimated by calculating  
 205 the difference between the total cropland area and the total area of 9 major crops.

$$206 \quad Raw\ data_{i+k} = \frac{Referenced\ trend_{i+k}}{Referenced\ trend_i} \times Raw\ data_i, \quad (1)$$

$$207 \quad Raw\ data_{i+k} = \frac{Referenced\ trend_{i+k} \times Raw\ data_i}{Referenced\ trend_i} \times \frac{k-i}{j-i} + \frac{Referenced\ trend_{i+k} \times Raw\ data_j}{Referenced\ trend_j} \times \frac{j-k}{j-i}, \quad (2)$$

208 Where *Raw data* is the raw data that contains missing values, *Referenced trend* is the complete data from  
 209 which the interannual variations that raw data can refer to, *i* and *j* are the beginning and ending year of the gap, *i + k*  
 210 is the *k*th missing year.

### 211 2.3 Spatializing county-level cropland density

212 By incorporating the county-level inventory (Section 2.2) and gridded cropland products, we reconstructed annual  
 213 cropland density maps with 1 km by 1 km resolution to represent the area and distribution of cultivated land in ~~the~~  
 214 ~~conterminous~~ US from 1850 to 2021. This process was divided into three periods: 2010-2021 (P2010), 1985-2009  
 215 (P1985), and 1850-1984 (P1850). CDL, LCMAP, and HYDE were used to provide the potential cropland distribution  
 216 in P2010, P1985, and P1850, respectively. For the initial density maps in P2010 and P1985, we used a 1 km window  
 217 to count cropland fraction in each grid resampled from the raw CDL and LMCAP (30m×30m), respectively, while  
 218 initial annual density maps in P1850 were resampled and linear interpolated from the HYDE maps. The pixel value  
 219 in the resampled density map, representing the proportion of the cultivated land over the total pixel area, was further  
 220 corrected based on the reconstructed county-level inventory data (Equation ~~(3)~~).

221 Specifically, when the total cropland area in a county from the initial density map is larger than that of the  
 222 inventory area, the extra area from all grid cells in the initial map would be deducted to keep consistent with the  
 223 magnitude of the inventory data; On the contrary, if the cropland area was less than the inventory data, the inadequate  
 224 area would be added to all pixels (Yu and Lu 2018). If the fraction in a grid is reduced below zero, the cropland  
 225 fraction in that grid is assigned to zero and the remaining difference area between the map and the inventory data is  
 226 subtracted from other grids. Conversely, if the fraction in a grid increases above one (100%), then the value in that  
 227 grid is assigned to one, and the remaining area will be added to other grids.

$$228 \quad AdjPixel_k = Pixel_k + \frac{(inv - \sum_i^m Pixel_k)}{n}, \quad (3)$$

229 Where *n* is the total number of valid cropland pixels in a county; *k* is the pixel ID in that county, which is from 1  
 230 to *n*; *inv* is the inventory crop area in that county; *Pixel<sub>k</sub>* is the initial cropland density in pixel *k*; *AdjPixel<sub>k</sub>* is the  
 231 adjusted cropland density in pixel *k*.

232 To eliminate the gap between CDL and LCMAP, we used the adjusted CDL 2010 density map as a baseline map  
 233 to retrieve the cropland density maps during 1985-2009 by adopting the year-to-year gridded changes from the

234 resampled LCMAP maps. Taking ~~developing the density map in~~ the year 2009 as an example, ~~we first calculated the~~  
 235 ~~annual/interannual~~ difference in each grid ~~from 2009 to 2010 based on the~~ ~~between~~ LCMAP density maps. Then, ~~we~~  
 236 ~~2009 and 2010 was~~ applied ~~that difference~~ to the adjusted CDL 2010 ~~map~~ to generate the potential crop density map  
 237 ~~in year 2009 with keeping the cropland area consistent with~~. Then, ~~the potential density map was further corrected by~~  
 238 the inventory area data through Equation 3. Following the same rule, the difference between the interpolated HYDE  
 239 1985 and 1984 was applied to the adjusted LCMAP 1985 ~~was used~~ to retrieve the density maps in P1850.

#### 240 2.4 Spatializing county-level crop type map

241 Based on the reconstructed county-level crop type inventory data (Section 2.2), corrected cropland density maps  
 242 (Section 2.3), and CDL, spatializing annual crop type maps was divided into two periods: 2010-2021 (P1) and 1850-  
 243 2009 (P2). For P1, the raw 30m resolution CDL crop type maps were resampled to 1 km to provide the potential crop  
 244 type distribution. In this process, we assigned the resampled grid to a type with the biggest percentage in a 1 km  
 245 window. By integrating resampled crop type maps and reconstructed cropland density maps, we counted the total area  
 246 for each type at the county level, and identified ~~specific~~ the crop types ~~with a whose area is~~ greater ~~area~~ than the  
 247 corresponding inventory data record. We further converted the surplus area pixels from these types to other types whose  
 248 area is less than inventory data (Equation 4 and 5). In particular, ~~considering the natural planting scenario to avoid a~~  
 249 grid planted by a fixed type for a long time, the surplus area was pixels are randomly selected for ~~converting to other~~ the  
 250 conversion across different crop types ~~to avoid a grid planted by a fixed type~~. For P2, we assumed that the crop type  
 251 pattern in two consecutive years wouldn't change significantly, and used the rebuilt crop type map in year<sub>*t+1*</sub> to provide  
 252 the potential crop type distribution in year<sub>*t*</sub>. Then, we followed the same rule in P1 to reconstruct the crop type map in  
 253 year<sub>*t*</sub>.

$$254 \text{AdjType}_j = \text{inv}_j - \sum_1^n (\text{AdjPixel}_{jk}), \quad (4)$$

255 Where  $j$  is the crop type ID ranging from 1 to 10, which is identified from the initial crop type map;  $n$  is the  
 256 number of total valid pixels in crop type  $j$ ;  $k$  is the pixel ID of crop type  $j$  ranging from 1 to  $n$  identified from the  
 257 initial crop type map;  $\text{inv}_j$  is the inventory area of type  $j$ ;  $\text{AdjPixel}_{jk}$  is the adjusted cropland percentage in pixel  $k$ ;  
 258  $\text{AdjType}_j$  is the crop area converted to other types; For year<sub>*t*</sub> between 2010 and 2021, the initial crop type map is  
 259 resampled from CDL; For year<sub>*t*</sub> from 1850 to 2009, crop type map is the adjusted crop type map in year<sub>*t+1*</sub>.

$$260 \begin{cases} \text{Converting the area of AdjType}_j \text{ from type } j \text{ to other types, if } \text{AdjType}_j < 0; \\ \text{Converting the area of AdjType}_j \text{ from other types to type } j, \text{ if } \text{AdjType}_j > 0; \end{cases} \quad (5)$$

261 ~~Considering the dominant crop rotation type in US, soybean and corn rotation, we simulated corn soybean~~  
 262 ~~rotation from 1940 to 2009 by randomly converting a certain area between corn and soybean according to the rotation~~  
 263 ~~rate. Based on CDL crop maps, we calculated the rotation rate as the ratio of the area where corn soybean conversion~~  
 264 ~~occurred to the total corn soybean area between the two consecutive years during 2010-2021 (Yu et al., 2018). To get~~  
 265 ~~a more reliable rotation rate, we did a rotation operation on the county where the corn soybean rotation occurred no~~  
 266 ~~less than seven years from 2010 to 2021 and assigned the average value as the rotation rate of the 2010s. Because~~  
 267 ~~soybean was rarely planted in the Corn Belt before 1940, we assumed that the rotation rate linearly increased from 0~~

268 in 1940 to that average value in 2010. Considering the dominant crop rotation type in US, soybean and corn rotation,  
 269 we simulated the corn-soybean rotation by randomly switching a certain area between corn and soybean according to  
 270 the rotation rate. The crop rotation information from 1996 to 2010 at state level was documented by the “Tailored  
 271 Reports: Crop Production Practices” of USDA’s Agricultural Resource Management Survey (ARMS)  
 272 (<https://data.ers.usda.gov/reports.aspx?ID=17883>). The rotation rate was calculated as the ratio of the sum of corn-  
 273 soybean and soybean-corn acreage to the total area of corn and soybean. We found that the rotation rate in each state  
 274 kept relatively stable in the ARMS-available years, and assumed that the rotation rate in the missing years is the same  
 275 as the mean rate from available years (Table S3), which is further applied to corresponding counties. Because soybean  
 276 was rarely planted in the Corn Belt before 1940 (Yu et al., 2018):

277 ~~Crop~~, we only considered the corn-soybean rotation during the period 1940-2009 in 17 states (Table S3) (Padgitt  
 278 et al., 1990).

279 **2.5 Evaluation method**

280 Here, we adopted multiple indexes to evaluate the crop area discrepancy between the reconstructed maps and  
 281 inventory data at various scales. At the county level, we utilized the residual ( $resd_{ij}$ ) and relative residual  
 282 ( $relative\_resd_{ij}$ ) to describe the crop area difference and relative difference between the rebuilt maps and the  
 283 inventory data (Equation 6 and 7). In addition, at the national scale, the Root Mean Squared Error (RMSE) and R-  
 284 squared ( $R^2$ ) are used to assess the crop area consistency between the crop maps and the inventory data.

285  $resd_{ij} = inv_{ij} - map_{ij}$ , (6)

286  $relative\_resd_{ij} = (inv_{ij} - map_{ij}) * 100 / inv_{ij}$ , (7)

287 Where,  $inv_{ij}$  and  $map_{ij}$  are the crop area derived from the inventory data and the rebuilt maps at year  $i$  and in  
 288 county  $j$ , respectively.  $resd_{ij}$  and  $relative\_resd_{ij}$  are the residue and relative residue at year  $i$  and in county  $j$ ,  
 289 respectively.

290 **2.5.2.6 Cropping diversity analysis**

291 ~~Crop~~Cropping diversity has been identified as a potential factor affecting crop yield (Renard and Tilman, 2019;  
 292 Driscoll et al., 2022). Here, we adopted a true diversity index proposed by Jost (2006)(2006) to analyze the US crop  
 293 diversity pattern. The true diversity ( $D$ ) quantifies the effective number of crop species (Equation 6), where a given  $D$   
 294 value is equivalent to ~~D~~the number of crop species occupying with an equal area in a certain space.  $D$  is calculated as  
 295 the exponent of Shannon diversity index ( $H$ ).

296 
$$D = \exp(-\sum_{j=1}^n (P_j * \ln P_j)) = \exp(H),$$
  
 297 (68)

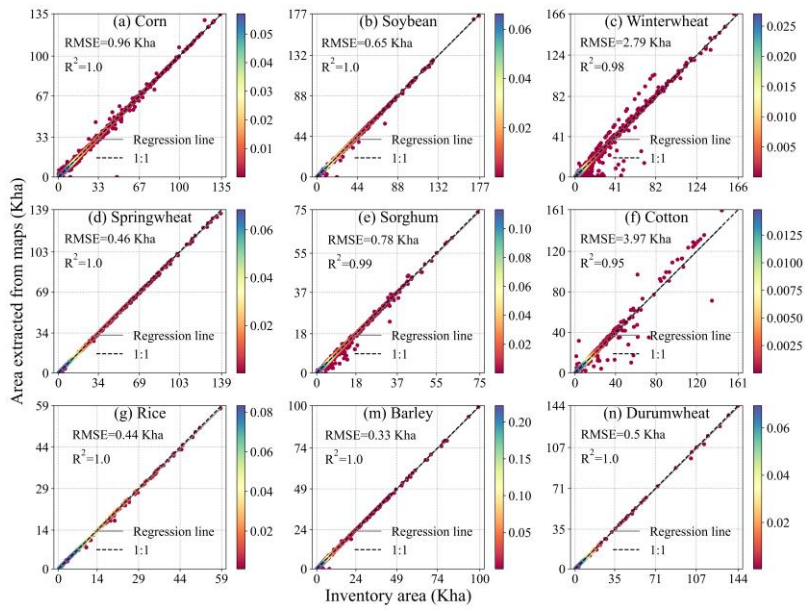
298 Where,  $P_j$  is the proportion of the cropland area occupied by crop type  $j$  over the total cropland area, and  $n$  is the  
 299 number of crop species. In this study, the diversity calculated involves ten crop types, including nine major crop types  
 300 and a category of “others”.

Formatted: Font: Not Italic

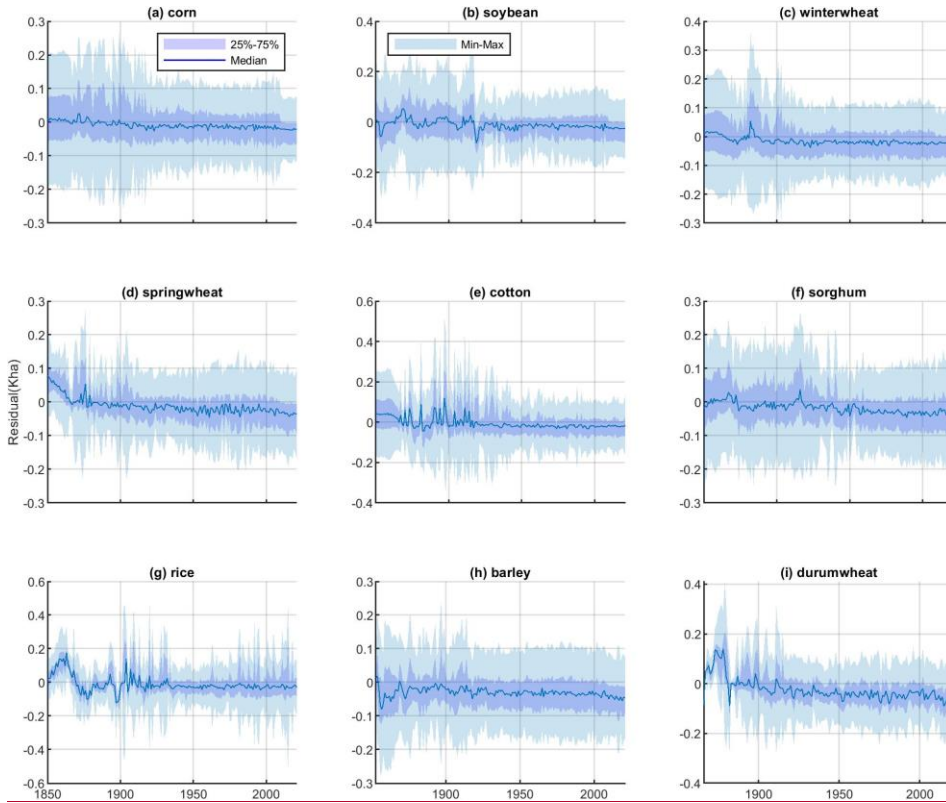
### 301 3 Result

#### 302 3.1 Validation of the data products

303 ~~To validate the developed maps, we~~ In this study, we adopted the inventory data to refine the gridded map,  
304 recognizing that achieving exact alignment for each crop type within each county might be challenging due to  
305 constraints related to the limited cropland area available for allocation. Here, we examined the crop-specific area  
306 alignment between the inventory data and our map products at multiple scales. We compared the annual crop type-  
307 specific acreage extracted from our maps with the raw inventory data at county level in 1920, 1960, 2000, and 2020  
308 (Figure ~~2S2~~). The county-level acreages derived from our products and inventory data are close to the 1:1 line, with  
309  $R^2$  exceeding 0.95 and  $RMSE < 1$  Kha for all the major crop types except for winter wheat ( $R^2 = 0.98$ ,  $RMSE = 2.79$   
310 Kha) and cotton ( $R^2 = 0.95$ ,  $RMSE = 3.97$  Kha). Although winter wheat and cotton present a relatively greater  $RMSE$ ,  
311 the counties with crop area bias greater than 10% only account for 9.7% and 6.1% of total winter wheat- and cotton-  
312 planting counties in the selected four years, respectively. We further examined the time-series residual between the  
313 inventory data and maps (Figure 2 and S3). It is evident that the residuals (the inventory-based crop area minus the  
314 rebuilt-map-based crop area (Equation 7)) are generally smaller than 0.2 Kha for the majority counties (>75%) across  
315 all years for nine crop types. Relatively greater residuals are observed in spring wheat, durum wheat, and rice before  
316 1875 (Figure 2d, g, and i), which might be attributed to the marginal area of these three crops during the early years.  
317 Similarly, the relative errors (the ratio of residual to the inventory crop area (Equation 8)) in most counties remain  
318 within  $\pm 2\%$  for different crops, except for spring wheat, durum wheat, and rice before 1875 (Figure S3d, g, and i). We  
319 also checked the consistency in national crop-specific acreage between our maps and the ~~rebuilt~~-inventory data during  
320 1850-2021 (Figure ~~S1S4~~). The results show that the map products match well with the inventory data ( $R^2$  close to 1  
321 and  $RMSE < 0.3$  Mha for all crop types), indicating that the developed maps are highly consistent with the inventory  
322 data at national scale. The multiple-scale validations ~~indicatedemonstrate~~ that the ~~cropland area from the~~ developed  
323 dataset ~~is highly reliable both at the national and county level.~~ has the strong capacity to capture the interannual crop-  
324 specific area variation.



325  
326



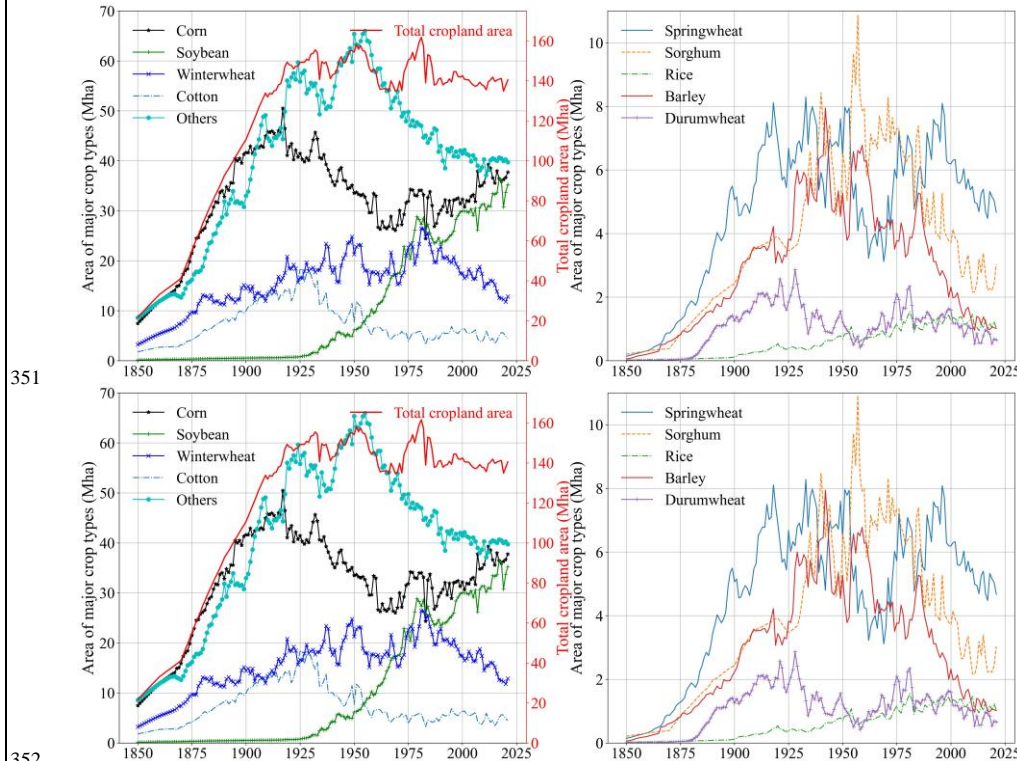
327  
 328 **Figure 2. Comparison** The distribution of residual (the inventory-based crop-specific cropland area - area minus the  
 329 rebuilt-map-based crop area, defined by Equation 6) between reconstructed the rebuilt inventory and maps and raw  
 330 inventory data at county level in 1920, 1960, 2000, and 2020 (from 1850 to 2021 (Kha is a thousand hectares). The  
 331 color bar in each subfigure indicates the probability density of paired-point calculated by the gaussian kernel. In each  
 332 year, "Min-Max", "Median", and "25%-75%" reflects the extent of residual from all counties at levels of "minimum  
 333 value to maximum value", "50th percentile", and "25th percentile to 75th percentile", respectively, which are  
 334 corresponding to five percentiles in a box plot.

335 **3.2 Temporal changes in crop-specific areas**

336 We examined the historical changes in cropland area changes among various crop types in the US from 1850 to  
 337 2021 (Figure 3). In general, the US cropland expanded rapidly from 21.7366 Mha in 1850 to 149.3828 Mha in 1919,  
 338 followed by a wide fluctuation ranging from 134.78 Mha to 161.80 Mha until 1990, and then kept relatively stable  
 339 around 140.00 Mha until 2021. Corn was the dominant crop in the US, accounting for more than 20% of the national  
 340 total cropland area throughout the study period. Temporally, it rose sharply from 7.47 Mha in 1850 to 50.5147 Mha  
 341 in 1917, followed by a continuous drop to 26.3426 Mha until 1962, and slowly increased to 37.75 Mha during 1962-  
 342 2021. Soybean soared significantly from 4.3835 Mha in the 1940s to 35.25 Mha in 2021, becoming the second most  
 343 extensive crop type in the US. Winter wheat constantly increased from 3.25 Mha in 1850 to 26.4843 Mha in 1981 and

Formatted: Normal, Left, Space After: 12 pt

344 then dropped to 12.88 Mha in 2021, while spring wheat fluctuated dramatically after it plateaued at 8.2928 Mha in  
 345 1933. Barley and sorghum climbed to peaks of around 8 Mha in 1940s and 11 Mha in 1950s, and then dropped to  
 346 about 1 Mha and 3 Mha by 2021, respectively. Besides, cotton and durum wheat both reached their peaks before the  
 347 1930s and then fell to a relatively stable level. Throughout the study period, the total US cropland increased by 118  
 348 Mha, predominantly driven by corn (30 Mha), soybean (35 Mha), and others (31 Mha). The remaining row crops  
 349 shared about 18% of this increase, including winter wheat (9.6 Mha), spring wheat (4.5 Mha), sorghum (2.78 Mha),  
 350 cotton (2.87 Mha), and rice (1 Mha).



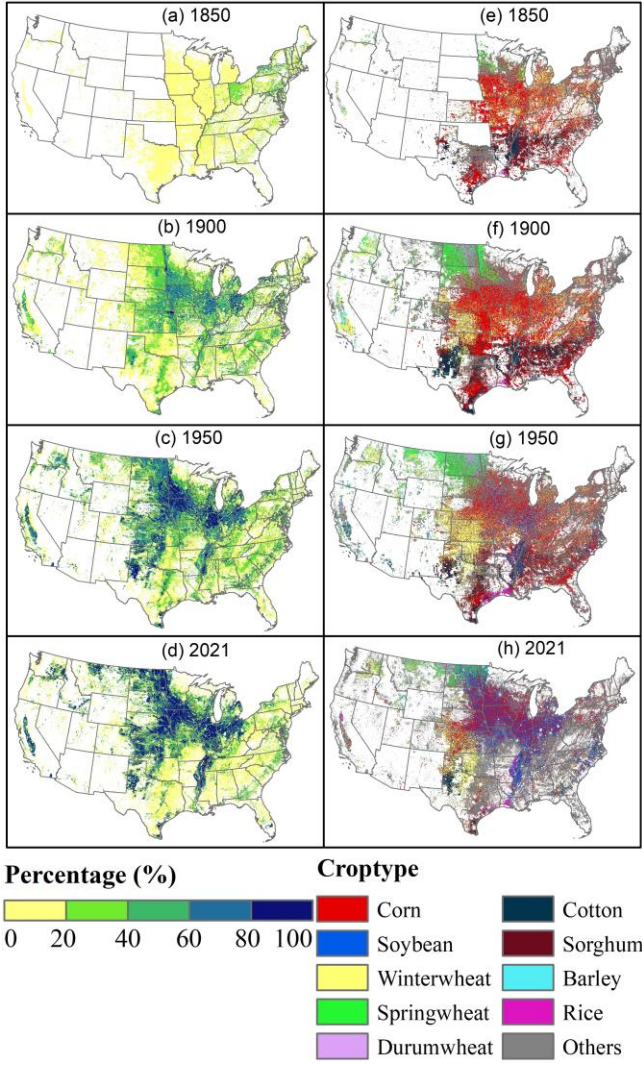
352  
 353 Figure 3. Annual area of major crop types and total US cropland area from 1850 to 2021.

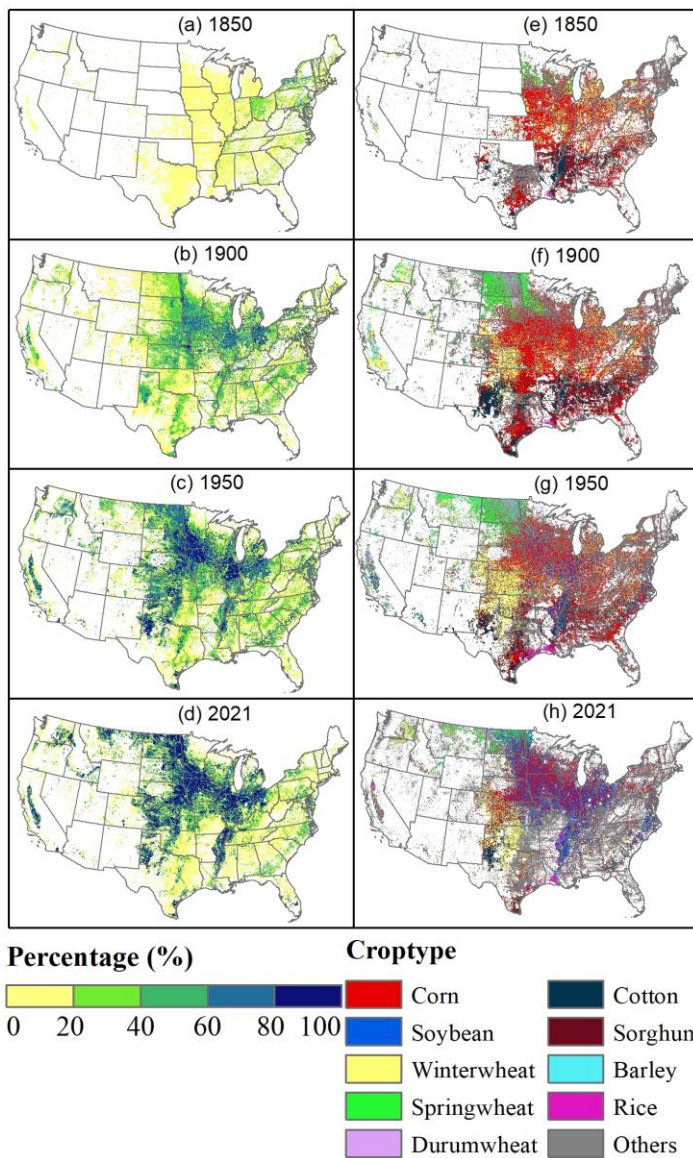
354 **3.3.3.2 Dynamics of cropland distribution**

355 The spatial patterns of cropland density and crop type are presented in Figure 4. Generally, the hotspots of  
 356 cropland are concentrated in the Midwest and Great Plains regions (the spatial pattern of US subregions showed in  
 357 Figure 5(2-a), starting from 1950, where large crop field sizes were likely to occur (Yan and Roy, 2016). The results  
 358 show that the cropland was mainly distributed in the eastern region of the US in 1850 with a low distribution  
 359 percentage (< 40%) (Figure 4(a)). Then, the cropland density enhanced substantially (40% -80%) in 1900 (Figure 4(b)).  
 360 Meanwhile, a large area of the Great Plains (the spatial pattern of US subregions showed in Figure 5(2-a)) was

361 cultivated to plant corn and spring wheat in the Northern Great Plains and winter wheat in the Southern Great Plains  
362 during 1850-1900 (Figure 4(f)). From 1900 to 1950, the cropland fraction was continuously elevated (>60%) (Figure  
363 4(c)), especially in the Midwest and the Great Plains. During 1950-2021, spring wheat expanded westward to Montana  
364 (Figure 4(h)), enhancing the cropland fraction in the Northern Great Plains. Moreover, the category of “others”  
365 substantially substituted corn, winter wheat, and cotton in the Southeast of US, and lowered the cropland density in  
366 this region (Figure 4(d)). It was noted that the soybean increased tremendously since 1950 in the Midwest, the Dakotas,  
367 and the rice belt, replacing parts of spring wheat, winter wheat, barley, and rice in these regions. Overall, the hotspots  
368 of US cropland have shifted from the Eastern US to the Midwest and the Great Plains with the increasing cropland  
369 percentage over the past 170 years.







371  
 372 Figure 4. The spatial patterns of cropland percentage (a-d) and crop type (e-h) at 1 km by 1km resolution in 1850,  
 373 1900, 1950, and 2021. The color bar of "Percentage" indicates the percentage of cultivated planting area to the grid  
 374 area. "Others" represents the remaining crop types.

375 Furthermore, the spatiotemporal patterns of each major crop type were examined in this study to present a  
 376 systematic understanding of the US cropland extent and type changes (Figure 5, Figure S2S5 and S3S6). Specifically,

377 corn was mainly planted in the east in 1850, with a low cropland fraction (<40%) (Figure 5(1-a)). Then, it gradually  
378 expanded to the Great Plains, and the total area increased by 40.3443 Mha from 1850 to 1917. Meanwhile, the hotspots  
379 of corn planting areas shifted to the Midwest, the southeast of the Northern Great Plains, and the northeast of the  
380 Southern Great Plains (Figure 5(1-b)). From 1917 to 1962, the spatial extent of corn had shrunk in South Dakota,  
381 Nebraska, Kansas, and the Southeast, with a total area decrease of 24.1721 Mha (Figure 5(1-c)). Although the  
382 Southeast experienced a large decline in corn acreage during 1962-2021, the planting density of corn significantly  
383 increased in the Midwest and the southeast of the Northern Great Plains, resulting in the corn area peaking at 37.75  
384 Mha in 2021 (Figure 5(1-d)).

385 Temporally, soybean was rarely cultivated in the US from 1850 to 1900 with a total area less than 1 Mha (Figure  
386 5 (2-a and 2-b)). During 1900-1940, the planting area of soybean had a small expansion in the Midwest, with a total  
387 area rising to 4.3835 Mha (Figure 5(2-c)). But then, it had a dramatic expansion from 1940 to 2021 to the Midwest,  
388 Southeast, and the east of Northern Great Plains, with the total soybean area increasing to 35.25 Mha (Figure 5(2-b)).

389 Winter wheat was mainly located in the Midwest in 1850 with a total area of 3.25 Mha (Figure 5(3-a)). In the  
390 following five decades, it spread to the Great Plains, California, Washington, and Oregon, with the total area increasing  
391 to 14.45 Mha in 1900 (Figure 5(3-b)). From 1900 to 1981, although its spatial extent had shrunk in Midwest, it  
392 expanded significantly in the Southern Great Plains, the Southeast, and Montana (Figure 5(3-c)). Meanwhile, the  
393 cropland density also enhanced in this period. These changes led to the planting area of winter wheat reaching the  
394 peak of 26.4843 Mha in 1981. However, during 1981-2021, a large area of winter wheat was replaced by other crop  
395 types or other land use types in the Midwest, Southeast, Montana, Washington, and California (Figure 5(3-d)), which  
396 reduced the total area of winter wheat to 12.88 Mha in 2021.

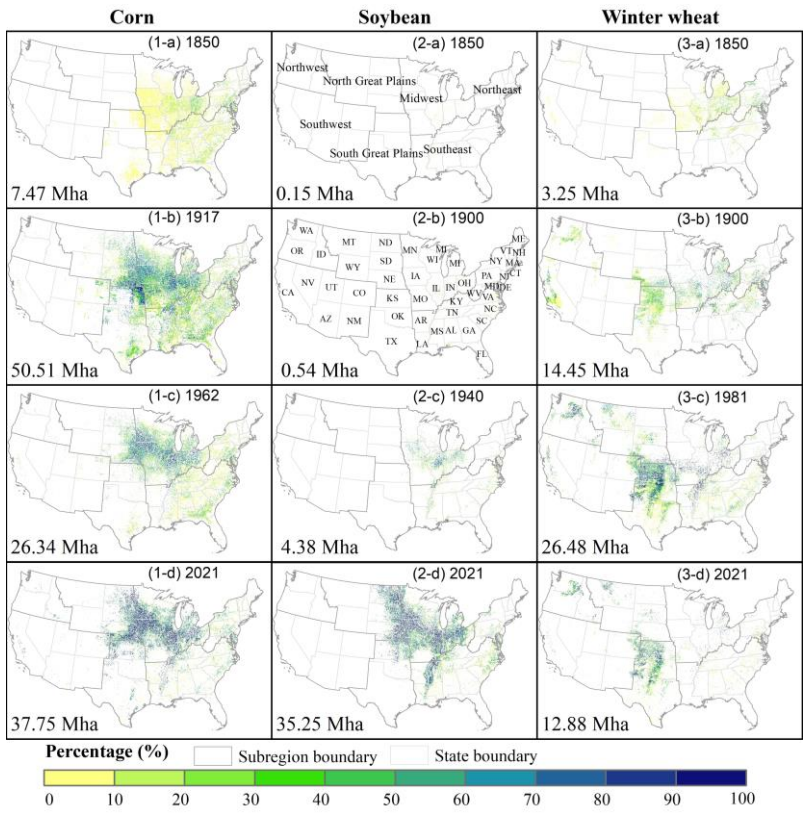
397 Cotton was mainly distributed in the Southeast in 1850 with a low density (Figure S2S5(1-a)). It sharply expanded  
398 to the Southern Great Plains and California with the increased density during 1850-1925 (Figure S2S5(1-b)), and the  
399 total area of cotton increased by 10.8016.53 Mha in this period. But the period of 1925-2021 was characterized by a  
400 huge contraction of cotton area in the Southeast and Southern Great Plains, with a total area declining to 4.50 Mha  
401 (Figure S2-S5(1-c and 1-d)).

402 For spring wheat, it significantly spread there was a significant expansion from Montana and Wisconsin to the  
403 Midwest and Northwest during 1850-1933, with the resulting in a total area increasing increase to 8.2928 Mha (Figure  
404 S2S5 (2-a) and (2-b)). But the distribution of spring wheat had largely shrunk in the Midwest and Northwest from  
405 1933 to 1969 (Figure S2S5 (2-b) and (2-c)), resulting in the area decreasing to 3.1211 Mha. In recent decades, it  
406 mainly centered in the northern part of the Northern Great Plains with the enhanced density in each grid, and its total  
407 area increased to 4.67 Mha in 2021 (Figure S2S5 (2-d)).

408 Sorghum consistently expanded in the Southern Great Plains from 1850 to 1957, and with its total area  
409 increased increasing by 10.6670 Mha (Figure S3S6 (1-a to 1-c)), followed by an). However, there was a subsequent  
410 area decline thereafter, which left leaving the total area at 3.03 Mha in 2021 (Figure S3S6 (1-d)). Similarly, barley  
411 experienced a continuous expansion in the Midwest, Great Plains, Northeast, California, and Colorado, with the total  
412 area rising from 0.06 Mha in 1850 to 7.94 Mha in 1942 (Figure S3S6 (2-b to 2-c)). However, between 1942 and 2021,

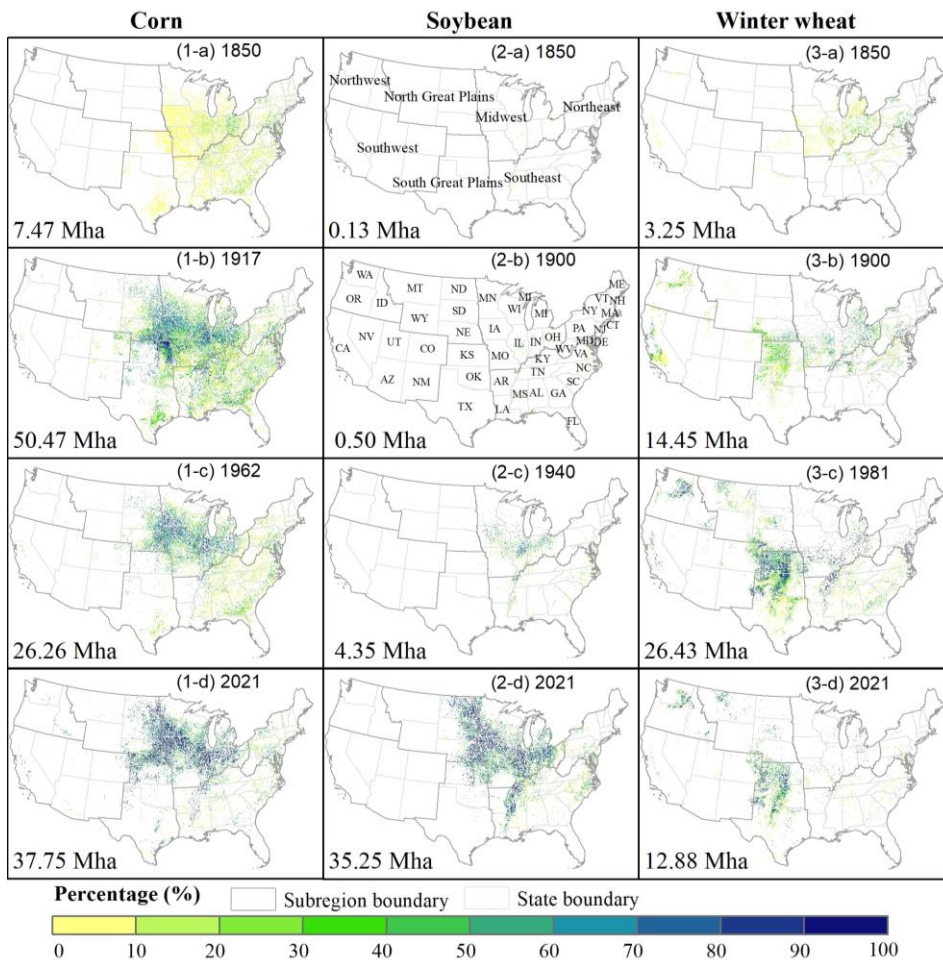
413 the distribution of barley had a dramatic contraction across the entire US and shrank to 1.02 Mha in 2021, with a small  
414 extent in the Northern Great Plains (Figure ~~S3S6~~ (2-d)).

415 Compared with other major crop types, both the distribution of durum wheat and rice only occupied a small area  
416 of the US over the entire study period (<3 Mha). Specifically, durum wheat ~~experienced a great~~underwent significant  
417 expansion in ~~the~~ North Dakota and South Dakota from 1850 to 1928 (Figure ~~S2S5~~ (3-a and 3-b)), ~~and its area~~  
418 ~~reached~~reaching a peak area of 2.8786 Mha in 1928. ~~However~~Subsequently, it contracted to the eastern part of North  
419 Dakota during 1928-1958, with a total area declining to 0.42 Mha (Figure ~~S2S5~~ (3-c)), ~~then~~). ~~From 1958 to 2021~~, its  
420 planting area shifted to the junction of North Dakota and Montana ~~from 1958 to 2021~~ (Figure ~~S2S5~~ (3-d)). Rice  
421 consistently expanded in Arkansas, Louisiana, Mississippi, and Texas from 1850 to 1981 ~~with~~, resulting in a total  
422 area increase of 1.5355 Mha (Figure ~~S3S6~~ (3-a to 3-c)). This expansion gradually ~~forming~~formed the current rice  
423 belt pattern, followed by a small shrinkage (0.52 Mha) in these regions between 1981 and 2021 (Figure ~~S3S6~~ (3-d)).  
424 The category of “others” includes ~~many other~~various minor crop types (~~such as~~ peanuts, oats, alfalfa, etc.), ~~which~~  
425 ~~accounts~~, collectively accounting for 27%~43% of the total US cropland area and ~~is distributed~~distributing across the  
426 entire US (Figure ~~S4S5~~).



427





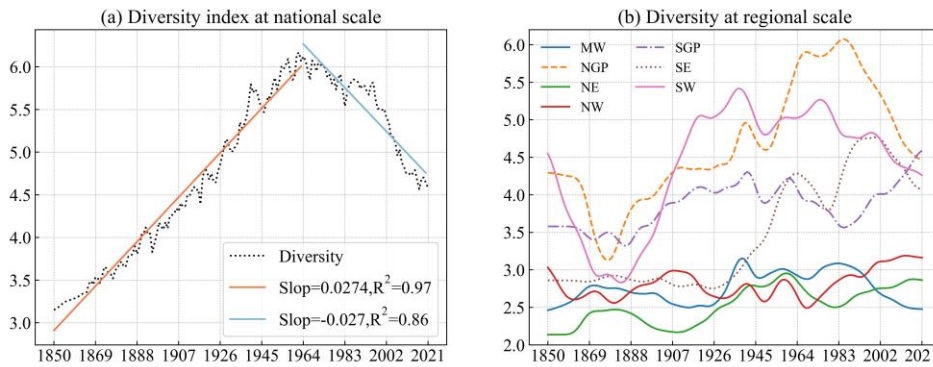
428  
429 Figure 5. The spatial density pattern of corn, soybean, and winter wheat at 1km by 1km resolution in the area turning  
430 years. The first, second, and third columns are the density pattern of corn, soybean, and winter wheat, respectively.  
431 The total planting area for each crop type is presented in the bottom left of each subfigure. The color bar at the bottom  
432 indicates the percentage of cultivated planting area to the total grid area.

Formatted: Font: 10 pt

433 **3.43.3 Changes in cropping diversity over time**

434 Here, the value of true diversity ( $D$ ) is interpreted as the number of crop species with an equal area in a certain  
435 space (L Jost, 2006; Hijmans et al., 2016)(L Jost, 2006; Hijmans et al., 2016), so a higher  $D$  value reflects more crop  
436 types, or more even distribution, or both. As shown in Figure 6, the US cropping system diversity had undergone  
437 dramatic change over time, with a sharp increase from 1850 to 1963 and a significant decline in the recent 60 years.  
438 Among different regions, the Southwest, Northern Great Plains, Southern Great Plains, and Southeast had a higher

439 cropping system diversity than the remaining regions. Specifically, the diversity in Southwest, Southern Great Plains,  
 440 and Northern Great Plains presented a similar change during 1850s-1940s, with a drop from 1850s to 1880s followed  
 441 by an obvious increase to 1940s (Figure 6 (b)). Starting from 1940s, the diversity in Northern Great Plains peaked  
 442 around 1990s and then constantly decreased to 2021, while Southern Great Plain's diversity presented an opposite  
 443 trend in this period. Meanwhile, Southwest witnessed a continuous decline in crop diversity from 1940s to now. The  
 444 Southeast kept its diversity stable during 1850s-1930s and then experienced a significant increase from 1940s to 2000s.  
 445 However, in the recent 20 years, the diversity in Southeast dropped sharply. The diversity in Northeast showed an  
 446 increase trend across the entire study period. Northwest's crop diversity fluctuated between 2.5 and 3 from 1850s to  
 447 1970s and then had a continuous increase to now. Midwest's crop diversity kept relatively stable during 1850s-1920s.  
 448 After increasing to its peak between 1920s and 1930s, it kept stable from 1930s to 1980s, followed by a dramatic  
 449 decrease to 2021.



450 Figure 6. The temporal trend of diversity value in US (a) and seven regions (b). NW, SW, NGP, SGP, MW, SE, and  
 451 NE are the abbreviation of Northwest, Southwest, Northern Great Plains, Southern Great Plains, Midwest, Southeast,  
 452 and Northeast, respectively. The spatial map of seven regions is presented in Figure 5 (2-b). To get a better visual  
 453 pattern, the trends of seven regions in (b) were smoothed by the gaussian function. The diversity value is calculated  
 454 based on the reconstructed inventory data.

## 456 4 Discussion

### 457 4.1 Comparison with other datasets

458 We ~~systematically compared the data products from this study and our product with~~ previous ~~works in terms~~  
 459 ~~of datasets regarding~~ the historical total cropland area ~~in the US~~ (Figure 7) and their spatial patterns (Figure 8) ~~to~~  
 460 ~~provide a complete reference for potential applications.~~ By combining NASS-CPAS and NASS-COA to reconstruct  
 461 state- and county-level inventory data, the US total cropland area derived from our density maps matches well with  
 462 that from NASS-CPAS from 1850 to 1940 and ~~aligns~~ consistently ~~aligns~~ with the magnitude of NASS-COA and the  
 463 interannual variations of NASS-CPAS between 1940 to 2021 (Figure 7). We extracted the US total cropland area from  
 464 two widely used geospatial satellite products (USDA-CDL and USGS-NLCD) in recent two decades. These two  
 465 datasets demonstrate a smaller area than that of NASS-~~CPASCOA~~ before 2017, ~~whereas the but their estimation of~~

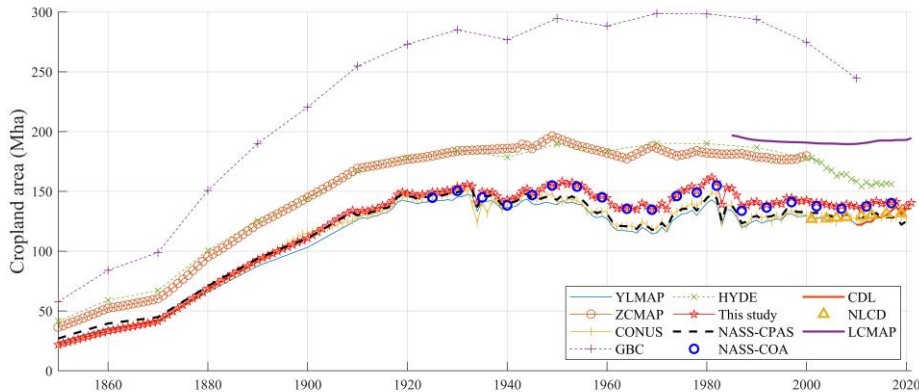
466 ~~crop area~~ magnitude and interannual variation ~~of their estimations were more consistent~~ have demonstrated greater  
467 ~~consistency~~ with this study ~~in~~ over the recent five years. Meanwhile, Yu and Lu (2018) and Li et al. (2023) all used  
468 NASS-CPAS to develop ~~YLMAP and CONUS~~ and ~~YLMAP~~, respectively, resulting in a lower US total cropland area  
469 after 1940 than this study. This is because the NASS-CPAS only includes the cropland area of principal crops in each  
470 state, which is lower than the total cropland area reported by NASS-COA, especially after 1940. Among the existing  
471 databases, LCMAP, HYDE, GBC, and ZCMAP represented an upper bound of the US total cropland area. Especially  
472 for GBC, it reported the national total crop acreage about 50% higher than the upper range of all other data products  
473 (~300 Mha vs ~200 Mha around the 1980s in Figure 7).

474 The divergence among these data products is mostly caused by different cropland definitions and cropland map  
475 generation processes. ~~Specifically~~ Spatially, we observed that HYDE exhibits broader cropland extent and a higher  
476 fraction of cropland per grid than our products, particularly in regions with low-density cropland distribution, such as  
477 the Northwest, Southeast, and Southwest (Figure 8 and Figure 9). This disparity might be attributed to the definition  
478 of cropland in HYDE, which includes both arable land and permeant cropland (Goldewijk, 2001) while our map  
479 exclusively accounts for crop planting area of crops. More importantly, the crop planting area of our map was  
480 constrained based on county level inventory data. Meanwhile, HDYE spatialized the subnational level inventory data  
481 to allocate cropland area to each grid in accordance with “cropland suitability maps” informed by dynamical social  
482 (historical population density) and stable environmental (soil suitability, temperature, and topography) information  
483 (Klein Goldewijk et al., 2011; Yu and Lu, 2018). As a result, greater acreage and wider extent of cropland were  
484 estimated by HYDE and were allocated to each grid (Figure 7, Figure S8, and Figure S9). Similarly, the category of  
485 cropland in LCMAP and ZCMAP contains crop and pasture (Zumkehr and Campbell, 2013; Xian et al., 2022), while  
486 the ~~GBC~~ cropland in HYDE and ~~GBC~~ includes ~~refers to~~ arable land (Goldewijk et al., 2017; Cao et al., 2021), leading  
487 to their higher cropland area than our result (Figure 7). Spatially, we found that the fraction in each grid from HYDE  
488 is higher in many low-density regions than our products, such as Northwest, Southeast, and Southwest (Figure 8 and  
489 the first row in Figure 9). This might be related to the weighting maps used to allocate cropland for each grid in HYDE,  
490 which heavily rely on social and natural indicators (Yu and Lu, 2018; Klein Goldewijk et al., 2011). Similarly, the  
491 ~~grid density of ZCMAP was also~~ Also, the grid density of ZCMAP was higher than this study in low-density regions  
492 (the first row in Figure 9) because ZCMAP adopted an assumption that the historical spatial crop pattern kept roughly  
493 similar to the basemap 2000, in which the fraction in each grid is higher in these regions (Ramankutty et al., 2008;  
494 Zumkehr and Campbell, 2013). Moreover, CONUS showed a more extensive cropland distribution than our maps  
495 (especially in the Great Plains and Southeast, Figure 8 and the third row in Figure 9). This is likely because they  
496 produced more potential cropland grids than the county records through an artificial neural networks-based land cover  
497 probability occurrence model (Li et al., 2023). GBC feeds population density and eight biophysical variables  
498 (including elevation, temperature, soil water, etc.) into a random forest model to generate the cropland distribution  
499 (Cao et al., 2021). As a result, the spatial pattern between GBC and our maps shows a high agreement at the national  
500 scale (Figure 8). However, the cropland percentage in each grid cell of GBC is significantly higher than other maps  
501 (Figure 8 and the second row in Figure 9), which might be related to the base map used in their study and the lack of  
502 inventory records for limiting the total cropland area in US (Cao et al., 2021).

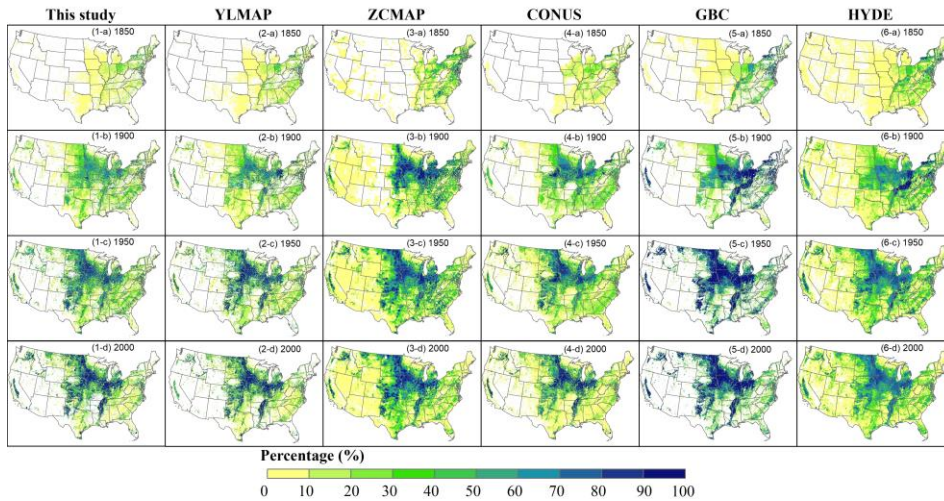


503 In terms of spatial details among these datasets, our products, YLMAP, CONUS, and GBC (1km×1km) can  
 504 provide more detailed spatial information than HYDE and ZCMPA (5 arc-min) (Figure 9). Furthermore, compared  
 505 with YLMAP, CONUS, and HYDE incorporating state-level census, our products are likely to demonstrate more  
 506 reliable cropland density heterogeneity within state (the third row in Figure 9) since we adopted county-level census  
 507 to control the total cropland area in each county. ~~Thus, the rebuilt map is capable of capturing spatial shifts between~~  
 508 ~~counties within a same state, such as cropland abandonment in some counties but expansion in others (Li et al.,~~  
 509 ~~2023); Thus, the rebuilt map is capable of capturing spatial shifts between counties within a same state, such as~~  
 510 ~~cropland abandonment in some counties but expansion in others (Figure 9).~~ This indicates that the county inventory-  
 511 derived datasets are more appropriate for subregion applications (Yang et al., 2020).

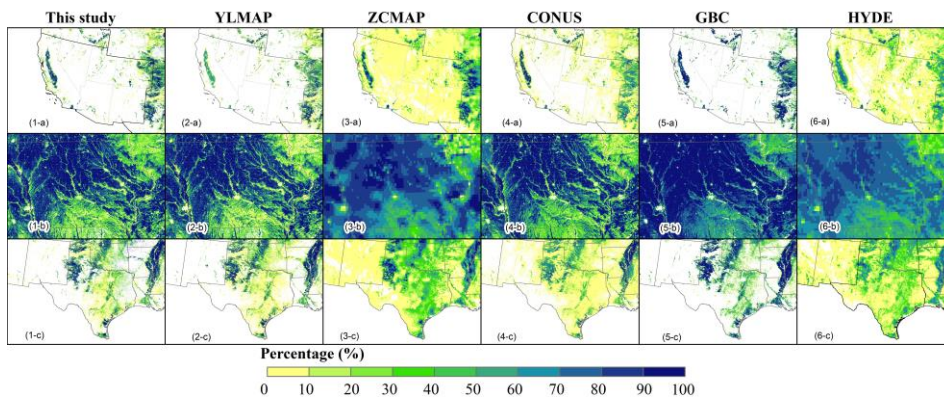
512 Overall, our product keeps highly consistent with the county-level inventory data and presents similar cropland  
 513 distribution to YLMAP and GBC that involves both biophysical and socioeconomic drivers to generate crop pixels.  
 514 In addition, unlike cropland involving arable land in HYDE or ~~harvest~~harvesting land in CONUS mentioned above,  
 515 the definition of cropland in our product refers to the ~~crop~~-planting ~~eropl~~and areas and excludes idle/fallow farm land  
 516 and cropland pasture, providing real surface information disturbed by agriculture. This ~~can improve~~improvement  
 517 ~~enhances~~ the ~~accuracy of estimating~~estimation cropland change's effect on the environment. Therefore, the developed  
 518 maps can provide a more comprehensive cropland tracking for ecological and environmental ~~applications~~assessment,  
 519 ~~covering~~ both ~~on the~~ cropland distribution and ~~eropl~~and area ~~crop types~~ at national and regional scales.



520 Figure 7. Comparison of the US total cropland area from different sources. CDL: Cropland data layer; NLCD: National  
 521 land cover database; LCMAP: Land change monitoring, assessment, and projection; YLMAP: the US cropland map  
 522 from Yu and Lu (2018); ZCMAP: the US cropland map from Zumkehr and Campbell (2013); CONUS: the cropland  
 523 map from Li et al.(2023); GBC: the US cropland extracted from the global cropland dataset developed by Cao et al.  
 524 (2021); HYDE: History database of the global environment 3.2 (Goldewijk et al., 2017); NASS-CPAS: the Crop  
 525 Production Annual Summary data from Nation agricultural statistical service of USDA; NASS-COA: the Census of  
 526 Agriculture from Nation agricultural statistical service of USDA. In particular, YLMAP, ZCMAP, CONUS, and GBC  
 527 are not used in this study.



529  
 530 Figure 8. The spatial patterns of cropland from different datasets in selected years of 1850, 1900, 1950, and 2000.  
 531 YLMAP (1km): the US cropland map from Yu and Lu (2018); ZCMAP (5 arc-min): the US cropland map from  
 532 Zumkehr and Campbell (2013); CONUS (1km): the cropland map from Li et al. (2023); GBC (1km): the US cropland  
 533 extracted from the global cropland dataset developed by Cao et al. (2021); HYDE (5 arc-min): History database of the  
 534 global environment 3.2 (Goldewijk et al. 2017).



535  
 536 Figure 9. The detailed spatial pattern from different datasets in the year 2000. YLMAP (1km): the US cropland map  
 537 from Yu and Lu (2018); ZCMAP (5 arc-min): the US cropland map from Zumkehr and Campbell (2013); CONUS  
 538 (1km): the cropland map from Li et al. (2023); GBC (1km): the US cropland extracted from the global cropland dataset  
 539 developed by Cao et al. (2021); HYDE (5 arc-min): History database of the global environment 3.2 (Goldewijk et al.  
 540 2017). The spatial extent in each row from (a) to (c) is Southwest, Iowa, and Texas, respectively.

541 **4.2 The drivers for US cropland change**

542 Between 1850 and 1900, there was a notable cropland expansion toward the west (Figure 4). This was mainly  
 543 driven by the Homestead Act of 1862, which provided 160 acres of land to the public for farming purposes (Anderson,

2011). Additionally, the end of the Civil War, the disbanding of armies, and the building of canals and railroads toward the west, further contributed to the agricultural market and export, accelerating agricultural reclamation (Ramankutty and Foley, 1999). At the same time, corn, cotton, and wheat were the dominant crop types and expanded rapidly to the west (Figure 5 and Figure S2). From 1900 to 1950, advanced irrigation systems, industrial technology, and mechanization further promoted agricultural development. For instance, the areas of winter wheat, sorghum, and barley increased substantially in this period (Figure 5 and Figure S2-S3). Subsequently, the fluctuation of the market, policy structure, and weather conditions played a dominant role in affecting the interannual variations of agricultural areas (Spangler et al., 2020). For example, the farm crisis of 1980s resulted in a significant cropland drop. Moreover, a series of historical acreage-reduction programs, such as the conservation adjustment act program, cropland acreage-reduction program, and conservation reserve program, resulted in the total cropland reduction (Lubowski et al., 2006). In the recent three decades, the total US cropland has kept relatively constant, but the crop commodities changed significantly. Corn and soybean gradually became the predominant types due to the rising demand for corn as biofuel and the higher market price for soybean, which pushed farmers to convert other types to corn and soybean (Bigelow and Borchers, 2017; Aguilar et al., 2015). Overall, the US cropland experienced significant growth between the 1850s and 1920s, driven by population growth, industrialization, mechanization, and market change. It subsequently underwent a process of stabilization after experiencing fluctuations in crop types and area.

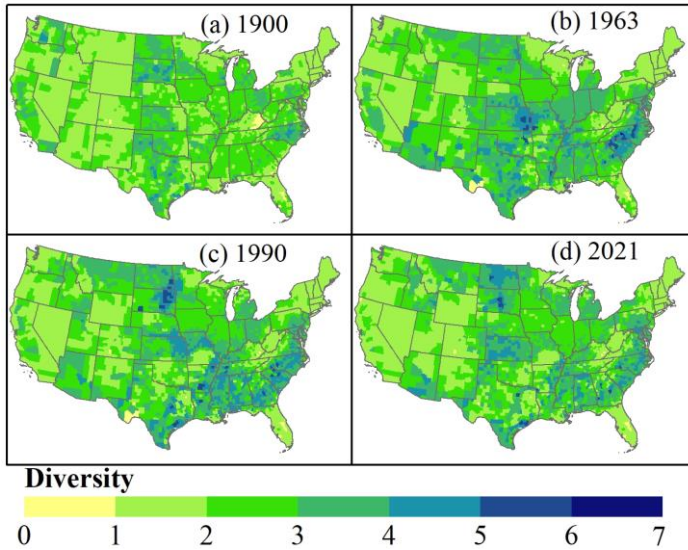
#### 4.3 The implications for cropping diversity change

In general, the US cropping diversity experienced a dramatic change throughout the entire period. From 1850 to 1963, it constantly increased (Figure 6 (a)), ~~which was~~ primarily attributed to the ~~area rises from rising areas of~~ all major crop types ~~at~~during this stage (Figure 3). Spatially, the diversity increases in ~~the~~ Southwest, Southeast, and Great Plains ~~promoted~~contributed to the ~~overall increase in US crop cropping~~ diversity ~~increase~~(Figure 6.(b) and 10). From 1960s to 2021, the cropping diversity had a significant decrease mainly due to the increased planting area for corn and soybean and the decreased cultivated area for winter wheat, spring wheat, sorghum, and barley. Meanwhile, the diversity drop in the Northern Great Plains, Southwest, Southeast, and Midwest might contribute to the US crop diversity decline (Figure 6 (b) and 10). This finding shows a strong agreement with the results of Aguilar et al. (2015), ~~in~~ which the crop species diversity declined from 1980s to 2010s in the Heartland Resource Region.

On the other hand, crop species diversity is an important component of biodiversity ~~in~~within a cropping system, and ~~the decreased a decrease in~~ crop species diversity ~~always accompanies the decreased~~is often associated with a ~~decline in overall~~ biodiversity (Altieri, 1999). Some researchers have pointed out that the biodiversity plays an essential role in the functioning of real-world ecosystem. High biodiversity would increase soil fertility, mitigate the impact of pests and diseases, improve resilience to climate change, and promote food production and nutrition security(Altieri, 1999; Duffy, 2009; Frison et al., 2011). For example, Delphine and David's research indicated that crop species diversity could stabilize food production (Renard and Tilman, 2019), and Emily et al. (2019) found that agricultural diversification can increase crop production. Thus, had this significant drop in the US cropping diversity in the past six decades affected yield and ecosystem productivity? Moreover, under more frequent climate extremes

Formatted: Default Paragraph Font, Font: 10 pt

579 anticipated in the future, whether the decreasing cropping diversity will affect the sustainability and resilience of the  
580 US agricultural system is an important question to answer.



581  
582 Figure 10. The spatial pattern of crop diversity in 1900, 1963, 1990, and 2021 at the county level. The diversity  
583 value is calculated based on the gap-filled and multi-source harmonized inventory data in each county.

#### 584 4.4 Uncertainty

585 In this study, we integrated the inventory data and the gridded LUCCLUC products to generate annual  
586 cropland density and crop type maps at a resolution of 1 km×1km from 1850 to 2021. Although our data is highly  
587 consistent with inventory data, some uncertainties remain:

588 (1) In the upscaling process of CDL from 30m to 1km, we assigned each pixel to a dominant crop type with the biggest  
589 fraction of land area within the pixel. Although the cropland area of each crop was constrained by the inventory data  
590 at the county level, this resampling process may ignore some overlook certain crop type distribution distributions with  
591 minor fraction within a pixel.

592 (2) The inventory is crucial for reconstructing historical cropland maps. Here, the rebuilt inventory data in missing  
593 years is interpolated, which might ignore some. Although this study is based upon our best knowledge and available,  
594 this method may not reflect the real interannual cropland area fluctuations, causing the final cropland map to  
595 misrepresent in the annual spatial cropland shift in these missing years.

596 (3) In the process of spatializing crop types, we randomly convert the cropland grids from specific types with higher  
597 cropland map area than inventory data to other crop types in within each county. Moreover, the In addition, grids  
598 identified to have with corn-soybean rotation were randomly selected within a county based on the corn-soybean  
599 rotation ratio, which can help avoid aiming to prevent a grid cell from being consistently occupied by a fixed single  
600 crop type over time. Although While the extent of the random processes varied among counties depending based on

601 the difference between intermediate map data and inventory data, ~~they might affect~~ it is important to note that they  
602 ~~may influence~~ the temporal trajectory of grid-based crop type changes. Thus, ~~the~~ users should ~~be cautious to~~  
603 ~~use~~ exercise caution when employing this data product ~~to conduct~~ for time sequencing analyses, such as crop rotation  
604 patterns (e.g., continuous corn, corn-soybean-corn, etc.) at the pixel level.

605 (4) The diversity in this study mainly reflects ~~ten crop types'~~ the change in diversity ~~change among ten crop types~~  
606 (nine major types and one category of "others"). ~~The~~ It is important to note that "others" in the study is not a single  
607 crop type, but a combined category including ~~many other~~ various minor crop types (peanuts, oats, etc.). Thus, the  
608 diversity ~~change~~ changes quantified in this study ~~reflect~~ capture the diversity of major row crops (accounting for 70%  
609 of the national total cropland area in the 2010s) and ~~the~~ "others-as-one-category" in the US over time. A more  
610 comprehensive diversity analysis involving all crop types ~~needs would require~~ a more detailed time-series crop type  
611 record, which is ~~currently~~ lacking ~~now~~.

## 612 5 Data availability

613 The developed dataset is available at <https://doi.org/10.6084/m9.figshare.22822838.v1> (Ye et al., 2023) ~~v2~~ (Ye et  
614 al., 2023). This dataset includes annual cropland density map and crop type map with Geotiff format at 1km by 1km  
615 spatial resolution.

## 616 6 Conclusion

617 In this study, the annual cropland density and crop type map from 1850 to 2021 in the conterminous US was  
618 developed by integrating the multi-source cross-scale inventory and gridded datasets. In general, our maps have a high  
619 consistency with inventory data both at the national level ( $R^2 > 0.99$ ,  $RMSE < 0.3$  Mha) and county level ( $R^2 > \text{the residual}$   
620 ~~less than 0.98, RMSE < 42~~ Kha for most counties (>75%)). Compared with other datasets, the spatial pattern of the  
621 developed maps matches well with YLMAP and GBC. Throughout the study period, the total US cropland increased  
622 by 118 Mha, mainly driven by corn (30 Mha), soybean (35 Mha), and others (31 Mha). The hot spots have shifted  
623 from the East to the Midwest and the Great Plains. Specifically, the Homestead Act of 1862 significantly contributed  
624 to the cropland expansion toward the west, and the rising demand for biofuel and the ~~elevated~~ market price resulted  
625 in the ~~dramatic~~ dramatic increase of corn and soybean planting areas. Meanwhile, the intensified corn and soybean  
626 substituted other crops, leading to the decrease of the cropping diversity in the Midwest, which may further influence  
627 crop yield and co-benefit of agroecosystem services. Additionally, there were random processes in generating crop  
628 type maps. This might bring uncertainty to pixel-based crop type sequence ~~applications~~ detection, but the area for each  
629 crop type was well constrained by gap-filled long-term inventory data- ~~at the county level~~. The county-level area  
630 control also ~~makes enables~~ the developed ~~map capable of depicting~~ maps to depict regional spatial shifts within state.  
631 Different from previous datasets, the cropland in our products refers to the planting area of all the crops, excluding  
632 idle/fallow farm land, and cropland pasture. Hence, the cropland map provides reliable cultivated information and  
633 reveals the surface disturbance conducted by agricultural activities, which can improve the estimation of cropland  
634 change's impact on climate ~~change~~ system. Overall, the developed datasets provide a historical cropland distribution

635 pattern ~~and fill~~, filling the data gap ~~in lacking~~ by providing long-term crop extent and type maps. We envision this  
636 database could better support the US agricultural management data development with crop-specific information, as  
637 well as improve the environmental assessment and socioeconomic analysis related to agriculture activities.



638 **Acknowledgments.** This work is supported partially by NSF grant (1903722), NSF CAREER (1945036), and USDA  
639 AFRI Competitive grant (1028219). [We appreciate the constructive comments and suggestions from two anonymous](#)  
640 [reviewers that have substantially improved the quality of this manuscript.](#)

641 **Author contributions:** CL designed the research; SC and PY implemented the research and analyzed the results; SC,  
642 PY, and CL wrote and revised the paper.

643 **Competing interests.** At least one of the (co-)authors is a member of the editorial board of Earth System Science  
644 Data.

## 645 **References**

- 646 Aguilar, J., Gramig, G. G., Hendrickson, J. R., Archer, D. W., Forcella, F., and Liebig, M. A.: Crop species  
647 diversity changes in the United States: 1978–2012, *PLoS One*, 10, 1–14, <https://doi.org/10.1371/journal.pone.0136580>,  
648 2015.
- 649 Aizen, M. A., Aguiar, S., Biesmeijer, J. C., Garibaldi, L. A., Inouye, D. W., Jung, C., Martins, D. J., Medel, R.,  
650 Morales, C. L., Ngo, H., Pauw, A., Paxton, R. J., Saez, A., and Seymour, C. L.: Global agricultural productivity is  
651 threatened by increasing pollinator dependence without a parallel increase in crop diversification, *Glob. Chang. Biol.*,  
652 25, 3516–3527, <https://doi.org/10.1111/gcb.14736>, 2019.
- 653 Altieri, M. A.: The ecological role of biodiversity in agroecosystems, *Agric. Ecosyst. Environ.*, 74, 19–31,  
654 [https://doi.org/10.1016/S0167-8809\(99\)00028-6](https://doi.org/10.1016/S0167-8809(99)00028-6), 1999.
- 655 Anderson, H. L.: That Settles It: The Debate and Consequences of the Homestead Act of 1862, *Hist. Teacher*, 45,  
656 117–137, 2011.
- 657 Arneth, A., Barbosa, H., Benton, T., Calvin, K., Calvo, E., Connors, S., Cowie, A., Davin, E., Denton, F., and  
658 van Diemen, R.: IPCC special report on climate change, desertification, land degradation, sustainable land  
659 management, food security, and greenhouse gas fluxes in terrestrial ecosystems, *Summ. Policy Makers*. Geneva  
660 Intergov. Panel Clim. Chang., 2019.
- 661 Betts, R. A., Falloon, P. D., Goldewijk, K. K., and Ramankutty, N.: Biogeophysical effects of land use on climate:  
662 Model simulations of radiative forcing and large-scale temperature change, *Agric. For. Meteorol.*, 142, 216–233,  
663 <https://doi.org/https://doi.org/10.1016/j.agrformet.2006.08.021>, 2007.
- 664 Bigelow, D. and Borchers, A.: Major uses of land in the United States, 2012, 2017.
- 665 Boryan, C., Yang, Z., Mueller, R., and Craig, M.: Monitoring US agriculture: the US Department of Agriculture,  
666 National Agricultural Statistics Service, Cropland Data Layer Program, *Geocarto Int.*, 26, 341–358,  
667 <https://doi.org/10.1080/10106049.2011.562309>, 2011.
- 668 Burchfield, E. K., Nelson, K. S., and Spangler, K.: The impact of agricultural landscape diversification on U.S.  
669 crop production, *Agric. Ecosyst. Environ.*, 285, <https://doi.org/10.1016/j.agee.2019.106615>, 2019.
- 670 Cao, B., Yu, L., Li, X., Chen, M., Li, X., Hao, P., and Gong, P.: A 1 km global cropland dataset from 10 000 BCE

671 to 2100 CE, *Earth Syst. Sci. Data*, 13, 5403–5421, <https://doi.org/https://doi.org/10.5194/essd-13-5403-2021>, 2021.

672 Driscoll, A. W., Leuthold, S. J., Choi, E., Clark, S. M., Cleveland, D. M., Dixon, M., Hsieh, M., Sitterson, J., and  
673 Mueller, N. D.: Divergent impacts of crop diversity on caloric and economic yield stability, *Environ. Res. Lett.*, 17,  
674 <https://doi.org/10.1088/1748-9326/aca2be>, 2022.

675 Duffy, J. E.: Why biodiversity is important to the functioning of real-world ecosystems, *Front. Ecol. Environ.*, 7,  
676 437–444, <https://doi.org/https://doi.org/10.1890/070195>, 2009.

677 Foley, J. A., DeFries, R., Asner, G. P., Barford, C., Bonan, G., Carpenter, S. R., Chapin, F. S., Coe, M. T., Daily,  
678 G. C., Gibbs, H. K., Helkowski, J. H., Holloway, T., Howard, E. A., Kucharik, C. J., Monfreda, C., Patz, J. A., Prentice,  
679 I. C., Ramankutty, N., and Snyder, P. K.: Global consequences of land use, *Science* (80-. ), 309, 570–574,  
680 <https://doi.org/10.1126/science.1111772>, 2005.

681 Frison, E. A., Cherfas, J., and Hodgkin, T.: Agricultural biodiversity is essential for a sustainable improvement  
682 in food and nutrition security, *Sustainability*, 3, 238–253, <https://doi.org/10.3390/su3010238>, 2011.

683 Gaudin, A. C. M., Tolhurst, T. N., Ker, A. P., Janovicek, K., Tortora, C., Martin, R. C., and Deen, W.: Increasing  
684 Crop Diversity Mitigates Weather Variations and Improves Yield Stability, *PLoS One*, 10,  
685 <https://doi.org/10.1371/journal.pone.0113261>, 2015.

686 Goldewijk, K. K.: [Estimating global land use change over the past 300 years: The HYDE database, \*Global\*](https://doi.org/10.1029/1999GB001232)  
687 [Biogeochem. Cycles, 15, 417–433, <https://doi.org/10.1029/1999GB001232>, 2001.](https://doi.org/10.1029/1999GB001232)

688 Goldewijk, K. K., Beusen, A., Doelman, J., and Stehfest, E.: Anthropogenic land use estimates for the Holocene  
689 - HYDE 3.2, *Earth Syst. Sci. Data*, 9, 927–953, <https://doi.org/10.5194/essd-9-927-2017>, 2017.

690 Hijmans, R. J., Choe, H., and Perlman, J.: Spatiotemporal Patterns of Field Crop Diversity in the United States,  
691 1870–2012, *Agric. Environ. Lett.*, 1, 160022, <https://doi.org/10.2134/ael2016.05.0022>, 2016.

692 Homer, C., Dewitz, J., Jin, S., Xian, G., Costello, C., Danielson, P., Gass, L., Funk, M., Wickham, J., Stehman,  
693 S., Auch, R., and Riitters, K.: Conterminous United States land cover change patterns 2001–2016 from the 2016  
694 National Land Cover Database, *ISPRS J. Photogramm. Remote Sens.*, 162, 184–199,  
695 <https://doi.org/https://doi.org/10.1016/j.isprsjprs.2020.02.019>, 2020.

696 Johnson, D. M.: A 2010 map estimate of annually tilled cropland within the conterminous United States, *Agric.*  
697 *Syst.*, 114, 95–105, <https://doi.org/10.1016/j.agry.2012.08.004>, 2013.

698 Klein-Jost, L.: [Entropy and diversity, \*Oikos\*](https://doi.org/10.1111/j.2006.0030-1299.14714.x), 113, 363–375, <https://doi.org/10.1111/j.2006.0030-1299.14714.x>,  
699 2006.

700 Goldewijk, K. K., Beusen, A., van Drecht, G., and de Vos, M.: The HYDE 3.1 spatially explicit database of  
701 human-induced global land-use change over the past 12,000 years, *Glob. Ecol. Biogeogr.*, 20, 73–86,  
702 <https://doi.org/https://doi.org/10.1111/j.1466-8238.2010.00587.x>, 2011.

703 L Jost: Entropy and ~~di~~-[iversity](https://doi.org/10.1111/j.2006.0030-1299.14714.x)diversity, *Opinion*, 2, 363–375, 2006.

704 Lambin, E. F. and Meyfroidt, P.: Global land use change, economic globalization, and the looming land scarcity,  
705 *Proc. Natl. Acad. Sci. U. S. A.*, 108, 3465–3472, <https://doi.org/10.1073/pnas.1100480108>, 2011.

706 Lark, T. J.: Interactions between U.S. biofuels policy and the Endangered Species Act, *Biol. Conserv.*, 279,  
707 109869, <https://doi.org/10.1016/j.biocon.2022.109869>, 2023.



708 [Lark, T. J., Mueller, R. M., Johnson, D. M., and Gibbs, H. K.: Measuring land-use and land-cover change using](#)  
709 [the U.S. department of agriculture's cropland data layer: Cautions and recommendations, \*Int. J. Appl. Earth Obs. Geoinf.\*, 62, 224–235, <https://doi.org/10.1016/j.jag.2017.06.007>, 2017.](#)

710

711 Li, X., Tian, H., Lu, C., and Pan, S.: Four-century history of land transformation by humans in the United States  
712 (1630–2020): annual and 1gkm grid data for the HIStory of LAND changes (HISLAND-US), *Earth Syst. Sci. Data*,  
713 15, 1005–1035, <https://doi.org/10.5194/essd-15-1005-2023>, 2023.

714 Lubowski, R. N., Vesterby, M., Bucholtz, S., Baez, A., and Roberts, M. J.: Major uses of land in the United States,  
715 2002, 2006.

716 Meinig, D. W.: *Shaping of America. Vol. 2, Continental America, 1800–1967: A Geographical Perspective on*  
717 *500 Years of History*, Yale University Press, 1993.

718 Monfreda, C., Ramankutty, N., and Foley, J. A.: Farming the planet: 2. Geographic distribution of crop areas,  
719 yields, physiological types, and net primary production in the year 2000, *Global Biogeochem. Cycles*, 22, 1–19,  
720 <https://doi.org/10.1029/2007GB002947>, 2008.

721 De Noblet-Ducoudré, N., Boisier, J. P., Pitman, A., Bonan, G. B., Brovkin, V., Cruz, F., Delire, C., Gayler, V.,  
722 Van Den Hurk, B. J. J. M., Lawrence, P. J., Van Der Molen, M. K., Müller, C., Reick, C. H., Strengers, B. J., and  
723 Voldoire, A.: Determining robust impacts of land-use-induced land cover changes on surface climate over North  
724 America and Eurasia: Results from the first set of LUCID experiments, *J. Clim.*, 25, 3261–3281,  
725 <https://doi.org/10.1175/JCLI-D-11-00338.1>, 2012.

726 Ouyang, W., Song, K., Wang, X., and Hao, F.: Non-point source pollution dynamics under long-term agricultural  
727 development and relationship with landscape dynamics, *Ecol. Indic.*, 45, 579–589,  
728 <https://doi.org/10.1016/j.ecolind.2014.05.025>, 2014.

729 [Padgitt, M., Newton, D., Penn, R., and Sandretto, C.: Production Practices for Major Crops in U.S. Agriculture,](#)  
730 [1990–97. Resource Economics Division, Economic Research Service, USDA., 1990.](#)

731 Ramankutty, N. and Foley, J. A.: Estimating historical changes in land cover North American croplands from  
732 1850 to 1992, *Glob. Ecol. Biogeogr.*, 8, 381–396, <https://doi.org/10.1046/j.1365-2699.1999.00141.x>, 1999.

733 Ramankutty, N., Evan, A. T., Monfreda, C., and Foley, J. A.: Farming the planet: 1. Geographic distribution of  
734 global agricultural lands in the year 2000, *Global Biogeochem. Cycles*, 22,  
735 <https://doi.org/https://doi.org/10.1029/2007GB002952>, 2008.

736 Renard, D. and Tilman, D.: National food production stabilized by crop diversity, *Nature*, 571, 257+,  
737 <https://doi.org/10.1038/s41586-019-1316-y>, 2019.

738 [Shi, W., Zhang, M., Zhang, R., Chen, S., and Zhan, Z.: Change Detection Based on Artificial Intelligence: State-](#)  
739 [of-the-Art and Challenges, \*Remote Sens.\*, 12, <https://doi.org/10.3390/rs12101688>, 2020.](#)

740 Spangler, K., Burchfield, E. K., and Schumacher, B.: Past and Current Dynamics of U.S. Agricultural Land Use  
741 and Policy, *Front. Sustain. Food Syst.*, 4, 1–21, <https://doi.org/10.3389/fsufs.2020.00098>, 2020.

742 Tang, F. H. M., Nguyen, T. H., Conchedda, G., Casse, L., and Tubiello, F. N.: CROPGRIDS: A global geo-  
743 referenced dataset of 173 crops circa 2020, 22491997, 1–22, 2023.

744 [Tian, H., Banger, K., Bo, T., and Dadhwal, V. K.: History of land use in India during 1880–2010: Large-scale](#)

745 [land transformations reconstructed from satellite data and historical archives, \*Glob. Planet. Change\*, 121, 78–88,](#)  
746 <https://doi.org/https://doi.org/10.1016/j.gloplacha.2014.07.005>, 2014.

747 Tilman, D., Balzer, C., Hill, J., and Befort, B. L.: Global food demand and the sustainable intensification of  
748 agriculture, *Proc. Natl. Acad. Sci. U. S. A.*, 108, 20260–20264, <https://doi.org/10.1073/pnas.1116437108>, 2011.

749 Turner, B. L.: The earth as transformed by human action, *Prof. Geogr.*, 40, 340–341, 1988.

750 Vanwalleghem, T., Gomez, J. A., Amate, J. I., de Molina, M. G., Vanderlinden, K., Guzman, G., Laguna, A., and  
751 Giraldez, J. V.: Impact of historical land use and soil management change on soil erosion and agricultural sustainability  
752 during the Anthropocene, *ANTHROPOCENE*, 17, 13–29, <https://doi.org/10.1016/j.ancene.2017.01.002>, 2017.

753 Waisanen, P. J. and Bliss, N. B.: Changes in population and agricultural land in conterminous United States  
754 counties, 1790 to 1997, *Global Biogeochem. Cycles*, 16, <https://doi.org/10.1029/2001GB001843>, 2002.

755 Xian, G. Z., Smith, K., Wellington, D., Horton, J., Zhou, Q., Li, C., Auch, R., Brown, J. F., Zhu, Z., and Reker,  
756 R. R.: Implementation of the CCDC algorithm to produce the LCMAP Collection 1.0 annual land surface change  
757 product, *Earth Syst. Sci. Data*, 14, 143–162, <https://doi.org/10.5194/essd-14-143-2022>, 2022.

758 [Yan, L. and Roy, D. P.: Conterminous United States crop field size quantification from multi-temporal Landsat  
759 data, \*Remote Sens. Environ.\*, 172, 67–86, <https://doi.org/10.1016/j.rse.2015.10.034>, 2016.](#)

760 Yang, J., Tao, B., Shi, H., Ouyang, Y., Pan, S., Ren, W., and Lu, C.: Integration of remote sensing, county-level  
761 census, and machine learning for century-long regional cropland distribution data reconstruction, *Int. J. Appl. Earth  
762 Obs. Geoinf.*, 91, 102151, <https://doi.org/10.1016/j.jag.2020.102151>, 2020.

763 Ye, S., Cao, P., and Lu, C.: Annual time-series 1-km maps of crop area and types in the conterminous US  
764 (CropAT-US) during 1850–2021, <https://doi.org/10.6084/m9.figshare.22822838.v1v2>, 2023.

765 Yu, Z. and Lu, C.: Historical cropland expansion and abandonment in the continental U.S. during 1850 to 2016,  
766 *Glob. Ecol. Biogeogr.*, 27, 322–333, <https://doi.org/10.1111/geb.12697>, 2018.

767 Yu, Z., Lu, C., Cao, P., and Tian, H.: Long-term terrestrial carbon dynamics in the Midwestern United States  
768 during 1850–2015: Roles of land use and cover change and agricultural management, *Glob. Chang. Biol.*, 24, 2673–  
769 2690, <https://doi.org/10.1111/gcb.14074>, 2018.

770 Zhang, W., Ricketts, T. H., Kremen, C., Carney, K., and Swinton, S. M.: Ecosystem services and dis-services to  
771 agriculture, *Ecol. Econ.*, 64, 253–260, <https://doi.org/https://doi.org/10.1016/j.ecolecon.2007.02.024>, 2007.

772 Zumkehr, A. and Campbell, J. E.: Historical U.S. cropland areas and the potential for bioenergy production on  
773 abandoned croplands, *Environ. Sci. Technol.*, 47, 3840–3847, <https://doi.org/10.1021/es3033132>, 2013.

774